

ORBIT: A Real-World Few-Shot Dataset for Teachable Object Recognition

Daniela Massiceti¹ Luisa Zintgraf² John Bronskill³ Lida Theodorou⁴

Matthew Tobias Harris⁴ Edward Cutrell¹ Cecily Morrison¹ Katja Hofmann¹ Simone Stumpf⁴

¹Microsoft Research ²University of Oxford ³University of Cambridge ⁴City, University of London

Abstract

Object recognition has made great advances in the last decade, but predominately still relies on many high-quality training examples per object category. In contrast, learning new objects from only a few examples could enable many impactful applications from robotics to user personalization. Most few-shot learning research, however, has been driven by benchmark datasets that lack the high variation that these applications will face when deployed in the real-world. To close this gap, we present the ORBIT dataset and benchmark, grounded in a real-world application of teachable object recognizers for people who are blind/low vision. The dataset contains 3,822 videos of 486 objects recorded by people who are blind/low-vision on their mobile phones, and the benchmark reflects a realistic, highly challenging recognition problem, providing a rich playground to drive research in robustness to few-shot, high-variation conditions. We set the first state-of-the-art on the benchmark and show that there is massive scope for further innovation, holding the potential to impact a broad range of real-world vision applications including tools for the blind/low-vision community. The dataset is available at <https://bit.ly/2OyEICj> and the code to run the benchmark at <https://bit.ly/39YgiUW>.

1. Introduction

Object recognition systems have made spectacular advances in recent years [43, 47, 44, 38, 14, 32, 37], however most systems still rely on training datasets with 100s to 1,000s of high-quality, labeled examples per object category. These demands make training datasets expensive to collect, and limit their use to all but a few application areas.

Few-shot learning aims to reduce these demands by training models to recognize completely novel objects from only a few examples [10, 49, 41, 54, 2, 39, 11, 46]. This opens the door to recognition systems that can adapt in real-world, dynamic scenarios, from self-driving cars to applications where users provide the training examples themselves. Meta-learning algorithms which “learn to learn” [45, 10, 49, 11]

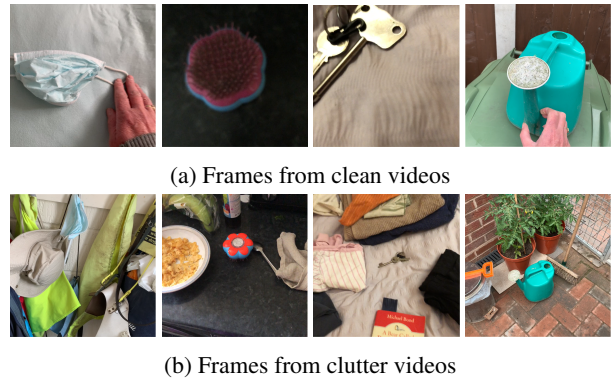


Figure 1: High-variation examples in the ORBIT dataset – a facemask, hairbrush, keys, and watering can. Full videos in the supplementary material. Further examples in Figure A.3.

hold particular promise towards this goal and recent advances have opened exciting possibilities for light-weight and adaptable recognition.

Most few-shot learning research, however, has been driven by datasets that lack the high variation that recognition systems will likely face when deployed in the real-world (for a dataset comparison see Table 1). Key datasets such as Omniglot [24, 49] and *miniImageNet* [49] present highly structured benchmark tasks which assume a fixed number of objects and training examples per object. Meta-Dataset [48] poses a more challenging benchmark task of adapting to a novel *dataset* given a small (random) number of training examples. Its constituent datasets [24, 17, 40, 28, 33, 50, 6], however, mirror the high-quality images of Omniglot and *miniImageNet*, leaving robustness to the noisy frames that would be streamed from a real-world system unaddressed. While these datasets have catalyzed research in few-shot learning, state-of-the-art performance is relatively saturated leaving less scope for algorithmic innovation [16, 4, 34].

To drive further innovation in few-shot learning for real-world impact, there is a strong need for datasets that capture the high variation inherent in real-world applications. We

motivate that both the dataset and benchmark task should be grounded in a potential real-world application to bring real-world recognition challenges to life in their entirety. An application area that neatly encapsulates a few-shot, high-variation scenario are teachable object recognisers (TORs) for people who are blind/low-vision [25, 18]. Here, a user can customize an object recognizer by capturing a small number of (high-variation) training examples of essential objects on their mobile phone. The recognizer is then trained on-the-fly on these examples such that it can recognize the user’s objects in novel scenarios. As a result, TORs present a microcosm of highly challenging and realistic conditions that can be used to drive research in real-world recognition tasks, with the potential to impact a broad range of applications beyond just tools for the blind/low-vision community.

We introduce the ORBIT dataset, a collection of videos recorded by people who are blind/low-vision on their mobile phones, and an associated few-shot benchmark grounded in realizing a TOR. Both were designed in collaboration with a team of machine learning (ML), human-computer interaction, and accessibility researchers, and will enable the ML community to 1) accelerate research in few-shot, high-variation recognition tasks, and 2) explore new research directions in few-shot *video* recognition tasks. We intend both as a rich playground to drive research in robustness to challenging, real-world conditions, a step beyond what curated vision datasets and structured benchmark tasks can offer, and to ultimately impact a broad range of real-world vision applications. In summary, our contributions are:

1. ORBIT benchmark dataset. The ORBIT benchmark dataset (Section 3) is a collection of 3822 videos of 486 objects recorded by 77 blind/low-vision people on their mobile phones and can be downloaded at <https://doi.org/10.25383/city.14294597>. Examples are shown in Figures 1 and A.3. Unlike existing datasets [40, 8, 28, 49, 48], ORBIT show objects in a wide range of realistic conditions, including when objects are poorly framed, occluded by hands and other objects, blurred, and in a wide variation of backgrounds, lighting, and object orientations.

2. ORBIT teachable object recognition benchmark. We formulate a few-shot benchmark on the ORBIT dataset (Section 4) that is grounded in TORs for people who are blind/low-vision. Contrasting existing few-shot (and other) works, the benchmark proposes a novel user-centric formulation which measures personalization to individual users. It also incorporates metrics that reflect the potential computational cost of real-world deployment on a mobile device. These and the benchmark’s other metrics are specifically designed to drive innovation for realistic settings.

3. State-of-the-art (SOTA) on the ORBIT benchmark. We implement 4 few-shot learning models that cover the main classes of approach in the field, extend them to videos,

and establish the first SOTA on the ORBIT benchmark (Section 5). We also perform empirical studies showing that training on existing few-shot learning datasets is *not* sufficient for good performance on the ORBIT benchmark (Table 5) leaving significant scope for algorithmic innovation in few-shot techniques that can handle high-variation data.

Code for loading the dataset, computing benchmark metrics, and running the baselines is available at <https://github.com/microsoft/ORBIT-Dataset>.

2. Related Work

Few-shot learning datasets. Omniglot [24, 49], *miniImageNet* [49], and Meta-Dataset [48] are 3 key datasets that have driven recent progress in few-shot learning. On Omniglot and *miniImageNet*, impressive accuracy gains have been achieved [49, 16, 4, 34], however results are now largely saturated and highly depend on the selected feature embedding. Meta-Dataset, a dataset of 10 datasets, formulates a more challenging task where whole *datasets* are held-out, but these datasets contain simple and clean images, such as clipart drawings of characters/symbols [24, 49, 17], and ImageNet-like images [28, 40, 33, 50, 6] showing objects in uniform lighting, orientations, and camera viewpoints. The ORBIT dataset and benchmark presents a more challenging, realistic few-shot task by using examples captured in high-variation conditions from real-world scenarios.

High-variation datasets. Datasets captured by users in real-world settings are naturally high-variation [1, 12, 7, 22, 29, 18, 42, 13], but none collected thus far explicitly target few-shot object recognition. *ObjectNet* [1] is a test-only dataset for “many-shot” classification containing challenging images (e.g. unusual orientations/backgrounds). *Something-Something* [12] and *EPIC-Kitchens* [7] are video datasets collected by users with mobile and head-mounted cameras, respectively, but are focused on action recognition based on many examples and “action captions”. *Core50* [29] is a video dataset captured on mobile phones for a continual learning recognition task. In contrast to ORBIT, the videos are high quality (captured by sighted people, with well-lit centered objects). High-variation datasets also include those collected by people who are blind/low-vision [18, 42, 13]¹, however, these are not appropriate for few-shot learning. *TeGO* [18] contains mobile phone images taken by only 2 users (1 sighted, 1 blind) in 2 environments (1 uniform background, 1 cluttered scene) of a set of 19 objects, and validates the TOR use-case, but is too small to deliver a robust, deployable system. *VizWiz* [13], although it contains 31,173 mobile phone images contributed by 11,045 blind/low-vision users, is targeted toward image captioning and question-answering tasks, and is not annotated with object labels. The ORBIT dataset and benchmark is motivated by the lack of existing

¹See *IncluSet*, a repository of accessibility datasets [19]

	Omniglot [24]	miniImageNet [49]	Meta-Dataset [48]	TEgO [25]	ORBIT Benchmark
Data type	Image	Image	Image	Image	Video frames
# classes	1623	100	4934	19	486
# samples/class	20	600	6-340,029	180-487	33-3,600
# total samples	32,460	60,000	52,764,077	11,930	2,687,934
Goal	Image classification	Image classification	Image classification	Image classification	Frame classification
Task	Fixed shot/way	Fixed shot/way	Random shot/way	Fixed shot/way	Random shot/way
Source	Turk	Web	Web	Mobile phone	Mobile phone
Data collectors	Sighted (20)	Sighted	Sighted	Sighted (1) Blind (1)	Blind (67)
High-variation features	Unbalanced classes	✗	✓	✗	✓
	Lighting variation	✗	✓	✓	✓
	Background variation	✗	✓	✓	✓*
	Viewpoint variation	✗	✗	✗	✓
	Ill-framed objects	✗	✗	✗	✓
	Blur	✗	✗	✗	✗

Table 1: Comparison of few-shot learning datasets. Note, the ORBIT benchmark dataset is a subset of all videos contributed by collectors (see Appendix B). *Collected in 2 controlled environments – 1 uniform background, 1 cluttered space.

datasets that have the scale and structure appropriate for a few-shot, high-variation real-world application, and adds to a growing repository of datasets for accessibility.

Few-shot applications. Few-shot learning has a wide range of possible applications, from recognizers that rapidly adapt to novel objects [20, 18], medical imaging tools that learn to classify/segment from a few scans [53, 27], and techniques that render talking faces [52] and 3D scenes/objects [9] from a few images. The application motivating this work are TORs for people who are blind/low-vision [18, 20].

3. ORBIT Benchmark Dataset

Our goal is to drive research in recognition tasks under few-shot, high-variation conditions so that deployed systems are robust in challenging, real-world scenarios. Toward this goal, we focus on a real-world application that serves as a microcosm of a few-shot, high-variation setting — TORs for people who are blind/low-vision – and engage the blind/low-vision community in collecting a large-scale dataset.

The collection took place in two phases, and collectors recorded and submitted all videos via an accessible iOS app (see Appendix A.2). The key design decision of capturing *videos* of objects was motivated by the fact that a video increases a blind collector’s chances of capturing frames that show the object well while reducing the time/effort cost to the collector, compared to multiple attempts at a single image. The study was approved by the City, University of London Research Ethics Committee and the data collection protocol is described in Appendix A.1

We summarize the benchmark dataset in Table 2 and describe it in detail below (see Appendix B for dataset preparation). It is used to run the ORBIT benchmark in Section 4. **Number of collectors.** Globally, 77 collectors contributed to the ORBIT benchmark dataset. Collectors who contributed only 1 object were merged to enforce a minimum of 3 objects per user such that the per-user classification task was a minimum of 3-way, resulting in an effective 67 users.

Numbers of videos and objects. Collectors contributed a total of 486 objects and 3,822 videos (2,687,934 frames, 83GB). 2,996 videos showed the object in isolation, referred to as *clean* videos, while 826 showed the object in a realistic, multi-object scene, referred to as *clutter* videos. We collected both types to match what a TOR will encounter (see Section 4.2.2). Each collector contributed on average 7.3 (± 2.8) objects, with 5.8 (± 3.9) clean videos and 1.8 (± 1.1) clutter videos per object. Figure 2 shows the number of objects (2a) and number of videos per collector (2b).

Types of objects. Collectors provided object labels for each video contributed. Objects covered course-grained categories (e.g. remote, keys, wallet) as well as fine-grained categories (e.g. Apple TV remote, Virgin remote control, Samsung TV remote control). We grouped the objects into clusters based on object similarity and observed a long-tailed distribution (see Figure A.6b). The largest clusters contained different types of remotes/controls, keys, wallets/purses, guidecanes, doors, airpods, headphones, mobile phones, watches, sunglasses and Braille readers. More than half of the clusters contained just one object. The clustering algorithm and cluster contents are included in Appendix D.

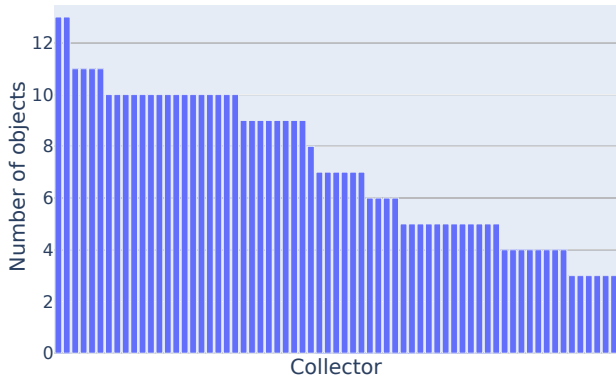
Object in-frame annotations. Frames from clutter videos for a subset of users were annotated with whether the object was fully in-frame, more than 50% in-frame, less than 50% in-frame, or not present at all (see Table 3). Annotations for the remaining users are underway. On average, the target object was more than half in-frame for $\sim 84\%$ of a given clutter video. Examples of clean and clutter frames are shown in Figure 1 with more examples in Appendix C.

Video lengths. Video lengths depended on the recording technique required for each video type (see Appendix A.1). On average, clean videos were 25.7s (~ 771 frames at 30 FPS), and clutter videos were 15.2s (~ 457 frames).

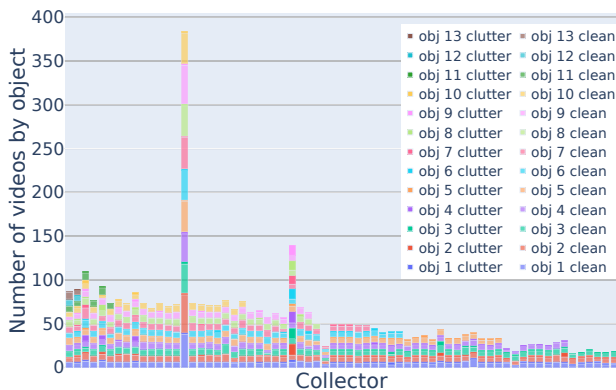
Unfiltered ORBIT dataset. Some users did not meet the minimum requirements to be included in the benchmark dataset (e.g. an object did not have both clean and clutter

	Collectors	Objects	Videos	Videos per object			Frames per video		
				mean/std	25/75 th perc.	min/max	mean/std	25/75 th perc.	min/max
Total	67	486	3822	7.9/4.8	7.0/7.0	3.0/46.0	703.3/414.1	396.2/899.0	33.0/3600.0
Clean			2996	6.2/4.6	5.0/6.0	2.0/44.0	771.3/420.6	525.8/900.0	33.0/3600.0
Clutter			826	1.7/1.5	1.0/2.0	1.0/13.0	456.7/272.9	248.5/599.0	40.0/3596.0
Per-collector	1	7.3/2.8	57.0/47.4	7.5/4.0	6.6/7.4	3.4/38.4	728.8/208.8	609.4/808.2	213.1/1614.3
Clean			44.7/44.0	5.8/3.9	4.8/6.0	2.4/36.5	809.9/244.7	664.7/898.5	219.3/1872.6
Clutter			12.3/10.8	1.8/1.1	1.0/2.0	1.0/9.9	728.8/208.8	609.4/808.2	213.1/1614.3

Table 2: ORBIT benchmark dataset.



(a) Number of objects per collector



(b) Number of videos (stacked by object) per collector

Figure 2: Number of objects and videos across 67 collectors

	Collectors	Clutter videos	Fully in-frame	$\geq 50\%$ in-frame	$< 50\%$ in-frame	Not present
Total	11	121	50.3 (31.6)	33.7 (25.4)	15.2 (17.5)	0.9 (3.9)
Per-collector	1	11.0 (1.9)	49.7 (15.2)	33.6 (10.1)	15.8 (9.9)	0.8 (1.2)

Table 3: Percentage of frames per video where the object is fully in-frame, more than half in-frame, less than half in-frame, and not present for clutter videos. Numbers reported as mean (standard deviation) over all clutter videos (first row) and over clutter videos per collector (second row)

videos). The benchmark dataset was therefore extracted from a larger set of 4733 videos (3,161,718 frames, 97GB) of 588 objects collected by 97 people who are blind/low-vision. We summarize the unfiltered dataset in [Appendix A.3](#).

4. Teachable Object Recognition Benchmark

The ORBIT dataset can be used to explore a wide set of real-world recognition tasks from continual learning [29, 30] to video segmentation [26, 35, 31]. In this paper, we focus on few-shot learning from high-variation examples and present a realistic and challenging few-shot benchmark grounded in the application of TORs for people who are blind/low-vision.

In [Section 4.1](#), we describe how a TOR works, mapping it to a few-shot learning problem, before presenting the benchmark’s evaluation protocol and metrics in [Section 4.2](#).

4.1. Teachable Object Recognition

We define a TOR as a generic recognizer that can be customized to a user’s personal objects, using a small number of training examples – in our case, videos – which the user has captured themselves. The 3 steps to realizing a TOR are:

- (1) **Train** A recognition model is trained on a large dataset of objects where each object has only a few examples. The model can be optimized to either i) directly recognize a set of objects [46, 5] or ii) learn *how* to recognize a set of objects (i.e. meta-learn) [10, 41, 49, 39]. This happens before deploying the model in the real world.
- (2) **Personalize** A real-world user captures a few examples of a set of their personal objects. The model is adapted to recognize this user’s objects using just these examples.
- (3) **Recognize** The user employs their now-personalized recognizer to identify their personal objects in novel (test) scenarios. As the user points their recognizer at a scene, it delivers frame-by-frame predictions.

4.1.1 TORs as a few-shot learning problem

The (1) **train** step of a TOR can be mapped to the ‘meta-training’ phase typically used in few-shot learning set-ups, and the (2) **personalize** and (3) **recognize** steps to ‘meta-testing’ (see [Figure 3](#)). With this view, we now formalize the teachable object recognition task, drawing on nomenclature from the few-shot literature [10, 41, 39, 11].

We construct a set of train users $\mathcal{K}^{\text{train}}$ and test users $\mathcal{K}^{\text{test}}$ ($\mathcal{K}^{\text{train}} \cap \mathcal{K}^{\text{test}} = \emptyset$) akin to the train and test object classes used in few-shot learning. A user κ has a set of personal objects \mathcal{P}^{κ} that they want a recognizer to identify, setting

up a $|\mathcal{P}^\kappa|$ -way classification problem. To this end, the user captures a few videos of each object, together called the user’s “context” set $\mathcal{C}^\kappa = \{(\bar{v}, p)_i\}_{i=1}^N$, where \bar{v} is a context video, $p \in \mathcal{P}^\kappa$ is its object label, and N is the total number of the user’s context videos. The goal is to use \mathcal{C}^κ to learn a recognition model f_{θ^κ} that can identify the user’s objects, where θ^κ are the model parameters specific to user κ .

The user can then point their personalized recognizer at novel “target” scenarios to receive per-frame predictions:

$$y_f^* = \arg \max_{y_f \in \mathcal{P}^\kappa} f_{\theta^\kappa}(v_f) \quad v_f \in \mathbf{v} \quad (\mathbf{v}, p) \in \mathcal{T}^\kappa \quad (1)$$

where v_f is a target frame, \mathbf{v} is a target video, \mathcal{T}^κ is all the user’s target videos, and $y_f \in \mathcal{P}^\kappa$ the frame-level label.²

Following the typical paradigm, during meta-training (i.e. the **train** step), multiple tasks are sampled per user $\kappa \in \mathcal{K}^{\text{train}}$ where a task is a random sub-sample of the user’s \mathcal{C}^κ and \mathcal{T}^κ (see Appendix F.2). The recognition model can be trained on these tasks using an episodic [10, 41, 49, 39] or non-episodic approach [5, 46, 23]. We formalize both in the context of TORs in Appendix E. Then, at meta-testing, one task is sampled per test user $\kappa \in \mathcal{K}^{\text{test}}$ containing *all* the user’s context and target videos. For each test user, the recognizer is personalized using all their context videos \mathcal{C}^κ (i.e. the **personalize** step), and then evaluated on each of the user’s target videos in \mathcal{T}^κ (i.e. the **recognize** step). In the following section, we discuss this evaluation protocol.

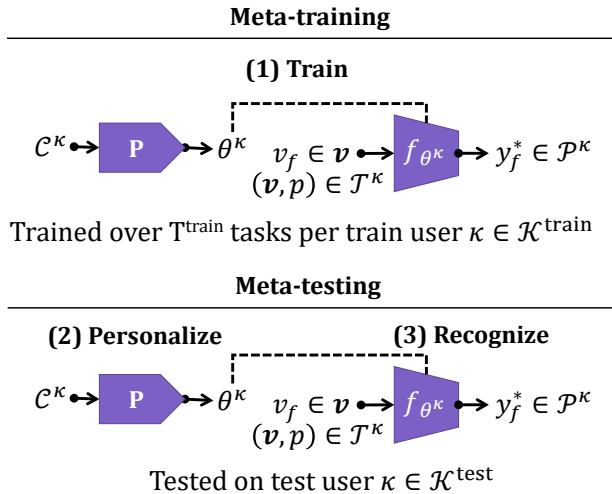


Figure 3: Teachable object recognizers cast as a few-shot learning problem. P is the personalization method, for example, several gradient steps using an optimization-based approach, or parameter generation using a model-based approach (see Section 5.1).

²Note, $y_f = p$ where $p \in \mathcal{P}^\kappa$ is the video-level object label

4.2. Evaluation protocol

ORBIT’s evaluation protocol is designed to reflect how well a TOR will work in the hands of a real-world user — both in terms of performance and computational cost to personalize. To achieve this, we test (and train) in a user-centric way where tasks are sampled *per-user* (that is, only from a given user’s objects and associated context/target videos). This contrasts existing few-shot (and other) benchmarks, and offers powerful insights into how well a meta-trained TOR can personalize to a single user.

4.2.1 Train/validation/test users

The user-centric formulation in Section 4.1.1 calls for a disjoint set of train users $\mathcal{K}^{\text{train}}$ and test users $\mathcal{K}^{\text{test}}$. We therefore separate the 67 ORBIT collectors into 44 train users and 17 test users, with the remaining 6 marked as validation users \mathcal{K}^{val} . To ensure the test case is sufficiently challenging, we enforce that test (and validation) users have a minimum of 5 objects (see further details in Appendix B.3). The total number of objects in the splits are 278/50/158, respectively. We report statistics for each set of train/validation/test users in Appendix C, mirroring those over all users in Section 3.

4.2.2 Evaluation modes

We establish 2 evaluation modes:

Clean video evaluation (CLE-VE). We construct a test user’s context set \mathcal{C}^κ from their clean videos, and target set \mathcal{T}^κ from a *held-out* set of their clean videos. This mode serves as a simple check that the user’s clean videos can be used to recognize the user’s objects in new ‘simple’ scenarios when the object is in isolation.

Clutter video evaluation (CLU-VE). We construct a test user’s context set \mathcal{C}^κ from their clean videos, and target set \mathcal{T}^κ from their clutter videos. This mode matches the real-world scenario when a user captures clean videos to register objects, and needs to identify those objects in complex, cluttered environments. We consider CLU-VE to be ORBIT’s primary evaluation mode since it most closely matches how a TOR will be used in the real-world.

4.2.3 Evaluation metrics

For a test user $\kappa \in \mathcal{K}^{\text{test}}$, we evaluate their personalized recognizer f_{θ^κ} on each of their target videos. We denote a target video of object $p \in \mathcal{P}^\kappa$ as $\mathbf{v} = [v_1, \dots, v_F]$, and its frame predictions as $\mathbf{y}^* = [y_1^*, \dots, y_F^*]$, where F is the number of frames and $y_f^* \in \mathcal{P}^\kappa$. We further denote y_{mode}^* as the video’s most frequent frame prediction. For a given target video, we compute its:

Frame accuracy : the number of correct frame predictions by the total number of frames in the video.

Frames-to-recognition (FTR) : the number of frames (w.r.t. the first frame v_1) before a correct prediction is made by the total number of frames in the video.

FRAME ACCURACY (\uparrow)

$$\frac{1}{|\mathcal{T}^{\text{all}}|} \sum_{(v,p) \in \mathcal{T}^{\text{all}}} \frac{\sum_{f=1}^{|\mathbf{v}|} \mathbb{1}[y_f^* = p]}{|\mathbf{v}|}$$

FRAMES-TO-RECOGNITION (\downarrow)

$$\frac{1}{|\mathcal{T}^{\text{all}}|} \sum_{(v,p) \in \mathcal{T}^{\text{all}}} \frac{\arg \min_{y_f^* \in \mathbf{v}} y_f^* = p}{|\mathbf{v}|}$$

VIDEO ACCURACY (\uparrow)

$$\frac{1}{|\mathcal{T}^{\text{all}}|} \sum_{(v,p) \in \mathcal{T}^{\text{all}}} \mathbb{1}[y_{\text{mode}}^* = p] \quad y_{\text{mode}}^* = \arg \max_{p \in \mathcal{P}^{\kappa}} \sum_{f=1}^{|\mathbf{v}|} \mathbb{1}[y_f^* = p]$$

Table 4: ORBIT evaluation metrics. Symbols \uparrow / \downarrow indicate up / down is better, respectively. \mathcal{T}^{all} is the set of all target videos pooled across all tasks for all test users in $\mathcal{K}^{\text{test}}$.

Video accuracy : 1, if the video-level prediction equals the video-level object label, $y_{\text{mode}}^* = p$, otherwise 0.

We compute these metrics for each target video in all tasks for all users in $\mathcal{K}^{\text{test}}$. We report the average and 95% confidence interval of each metric over this flattened set of videos, denoted \mathcal{T}^{all} (see equations in Table 4).

We also compute 2 computational cost metrics:

MACS to personalize : number of Multiply-Accumulate operations (MACS) to compute a test user’s personalized parameters θ^{κ} using their context videos \mathcal{C}^{κ} , reported as the average over all tasks pooled across test users.

Number of parameters : total parameters in recognizer.

We flag frame accuracy as ORBIT’s primary metric because it most closely matches how a TOR will ultimately be used. The remaining metrics are complementary: FTR captures how long a user would have to point their recognizer at a scene before it identified the target object, with fewer frames being better, while video accuracy summarizes the predictions over a whole video. MACS to personalize provides an indication whether personalization could happen directly on a user’s device or a cloud-based service is required, each impacting how quickly a recognizer could be personalized. The number of parameters determines the storage and memory requirements of the model on a device, and if cloud-based, the bandwidth required to download the personalized model. It is also useful to normalize performance by model capacity.

5. Experimental analyses and results

5.1. Baselines & training set-up

Baselines. There are 3 main classes of few-shot learning approaches. In *metric-based* approaches, a per-class embedding is computed using the (labeled) images in the training examples, and a target image is classified based on its distance to each [41, 49]. In *optimization-based* approaches, the model takes many [51, 46, 5] or few [10, 54, 2] gradient steps on the context images, and the updated model then classifies the target image. Finally, in *model-based* approaches, the model uses the context images to directly generate the parameters of the classifier which is then used to classify the target image [39, 11].

We establish baselines on the ORBIT dataset across these main classes. Within the episodic approaches, we choose Prototypical Nets [41] for the metric-based family, MAML [10] for the optimization-based family, and

CNAPs [39] for the model-based family. We also implement a non-episodic fine-tuning baseline following [46, 5] who show that it can rival more complex methods. This selection of models offers good coverage over those that are competitive on current few-shot learning image classification benchmarks. For descriptions of these baselines and all implementation details see Appendix F.1.

Video representation. In Section 4.1.1, tasks are constructed from the context and target videos of a given user’s objects. We sample clips from each video and represent each clip as an average over its (learned) frame-level features. For memory reasons, we do not sample all clips from a video. Instead, during meta-training, we randomly sample S^{train} non-overlapping clips, each of L contiguous frames, from both context and target videos. Each clip is averaged, and treated as an ‘element’ in the context and target sets, akin to an image in a typical few-shot image classification pipeline. During meta-testing, however, following Section 4.2 and Eq. (1), we must evaluate a test user’s personalized recognizer on *every* frame in *all* of their target videos. We, therefore, sample *all* overlapping clips in a target video, where a clip is an L -sized buffer of each frame plus its short history. Ideally, this should also be done for context videos, however, due to memory reasons, we sample S^{test} non-overlapping L -sized clips from each context video, similar to meta-training. In our baseline implementations, $S^{\text{train}} = 4$, $S^{\text{test}} = 8$, and $L = 8$ (for further details see Appendices F.2 and F.3).

How frames are sampled during training/testing, and how videos are represented is flexible. The evaluation protocol’s only strict requirement is that a model outputs a prediction for every frame from every target video for every test user.

Number of tasks per test user. Because context videos are sub-sampled during meta-testing, a test user’s task contains a random set, rather than *all*, context clips. To account for potential variation, therefore, we sample 5 tasks per test user, and pool all their target videos into \mathcal{T}^{all} for evaluation. If memory was not a constraint, following Section 4.1.1, we would sample one task per test user which contained *all* context and *all* target clips.

5.2. Analyses

Baseline comparison. Performance is largely consistent across the baseline models in both CLE-VE and CLU-VE modes (see Table 5). In CLE-VE, all methods are equivalent in frame and video accuracy, except for ProtoNets which

MODEL	Clean Video Evaluation (CLE-VE)				Clutter Video Evaluation (CLU-VE)				METHOD TO PERSONALIZE	# PARAMS
	FRAME ACC	FTR	VIDEO ACC	MACS TO PERSONALIZE	FRAME ACC	FTR	VIDEO ACC	MACS TO PERSONALIZE		
ProtoNets [41]	62.19 (2.12)	8.36 (1.38)	76.73 (2.88)	2.88×10^{12}	51.10 (1.70)	15.40 (1.45)	60.73 (2.47)	3.53×10^{12}	1 forward pass	11.18M
CNAPs [39]	66.37 (2.18)	6.63 (1.25)	78.42 (2.81)	3.16×10^{12}	49.76 (1.86)	18.78 (1.71)	55.73 (2.51)	3.87×10^{12}	1 forward pass	12.76M
MAML [10]	68.24 (2.24)	9.62 (1.78)	78.55 (2.80)	69.76×10^{12}	51.67 (1.86)	19.74 (1.76)	57.47 (2.50)	82.39×10^{12}	15 gradient steps	11.18M
FineTuner [46, 5]	68.30 (2.34)	10.54 (1.85)	77.94 (2.83)	232.52×10^{12}	52.52 (1.88)	18.60 (1.76)	58.00 (2.50)	274.62×10^{12}	50 gradient steps	11.18M

Table 5: Baselines on the ORBIT Dataset. Results are reported as the average (95% confidence interval) over all target videos across all tasks for 17 test users.

trails slightly in frame accuracy. CNAPs is the fastest to make a prediction (i.e. lowest FTR). Comparing this to CLU-VE, we see overall performance drops of 10-15 percentage points. Here, all models are equivalent on frame accuracy, and ProtoNets ranks first in both FTR and video accuracy. Further, absolute CLU-VE scores are in the low 50s. Casting back to Table 3 where the object is more than half in-frame for $\sim 84\%$ of any given clutter video, this suggests that there is ample scope for improvement and motivates the need for approaches that can handle distribution shifts from clean (context) to real-world, cluttered scenes (target), and are robust to high-variation data more generally.

In computational cost, ProtoNets has the lowest cost to personalize with only a single forward pass of a user’s context videos, while FineTuner has the highest, requiring 50 gradient steps. This, along with the total number of parameters (which are similar across models), suggests that ProtoNets and CNAPs would be better suited to deploying a TOR on a mobile device.

Meta-training on other few-shot learning datasets. A model meta-trained on any dataset should, in principle, have the ability to learn *any* new object with only a few examples. We investigate this by meta-training on Meta-Dataset [48] using its standard task sampling protocol and then testing them on the ORBIT dataset (i.e. personalizing to test users with no training). We adapt the meta-trained models to videos by taking the average over frame features in clips sampled from context and target videos (see Section 5.1). In Table 6, CLE-VE and CLU-VE performance across all metrics is significantly lower than the corresponding baselines in Table 5. MAML and CNAPs perform particularly poorly while ProtoNets and FineTuner fare slightly better, however, are still ~ 10 percentage points below their above counterparts. This supports the idea that even though much progress has been made on existing few-shot benchmarks, they are not representative of real-world conditions and models trained on them may struggle to learn new objects with real-world, high-variation examples.

Per-user performance. In addition to averaging over \mathcal{T}^{all} , our user-centric paradigm allows us to average *per-user* (i.e. over just their target videos, then their tasks) This is important because it reflects how well a meta-trained TOR would personalize to each and *all* users in the real-world. In Figure 4, we see that ProtoNet’s personalization is not consistent

MODEL	FRAME ACC	FTR	VIDEO ACC
ProtoNets [41]	54.97 (2.33)	13.50 (1.99)	68.36 (3.17)
CNAPs [39]	45.35 (2.60)	26.72 (2.67)	53.09 (3.41)
MAML [10]	28.64 (2.65)	53.94 (3.27)	30.79 (3.15)
FineTuner [46, 5]	56.46 (2.37)	13.97 (2.06)	70.42 (3.11)

Table 6: CLE-VE performance when meta-training on Meta-Dataset and meta-testing on ORBIT (for CLU-VE see Appendix G). Even on clean videos, models perform poorly compared to when meta-training on ORBIT (Table 5) suggesting that existing few-shot datasets may be insufficient for real-world adaptation.

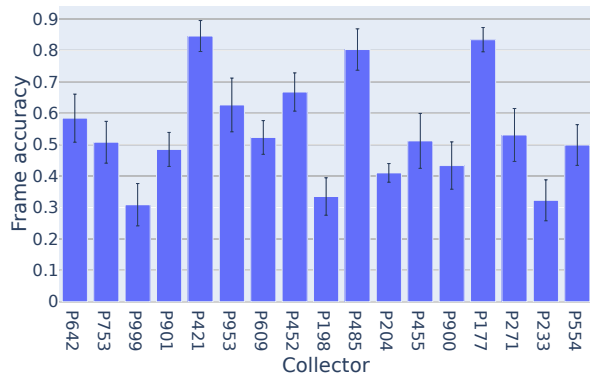


Figure 4: Frame accuracy varies widely across test users (error bars are 95% confidence intervals) on CLU-VE with ProtoNets [41]. For other metrics and models see Figure A.9.

across users, for some users going as low as 30% in frame accuracy (for other metrics and models, see Figure A.9). A TOR should be able to adapt to *any* real-world user, thus future work should equally aim to boost performance on the benchmark metrics *and* reduce variance across test users.

Train task composition. Finally, we investigate the impact of the number of context videos per object (Figure 5), and the number of objects per user (Figure 6) sampled in train tasks on CLU-VE frame accuracy. In the first case, we expect that with more context videos per object, the more diversity the model will see during meta-training, and hence generalize better at meta-testing to novel (target) videos. To test this hypothesis, we fix a quota of 96 frames per object in each

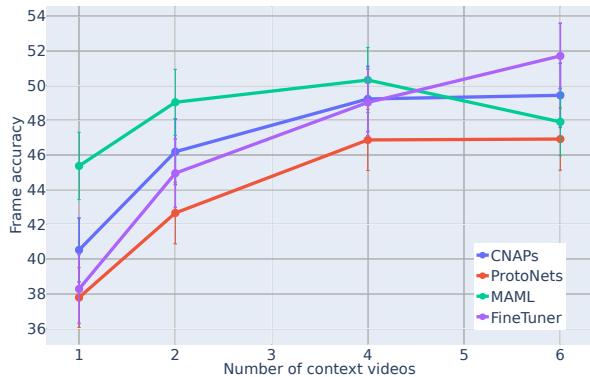


Figure 5: Meta-training with more context videos per object leads to better CLU-VE performance. Frames are sampled from an increasing number of clean videos per object using the number of clips per video (S^{train}) to keep the total number of context frames fixed in train tasks.

train task, and sample these frames from increasing numbers of context videos. Frame accuracy increases with more context videos, but overall plateaus between 4-6 context videos per object. Looking at the number of objects sampled per user next, we cap all train user’s objects at $\{2, 4, 6, 8\}$, respectively, when meta-training. We then meta-test in two ways: 1) we keep the caps in place on the test users, and 2) we remove the caps. For 1), we see reducing accuracy for increasing numbers of objects, as is expected – classifying between 8 objects is harder than classifying between 2. For 2), we see a significant drop in accuracy relative to 1) suggesting that meta-training with fewer objects than would be encountered at meta-testing is detrimental. This is an important real-world consideration since it is likely that over months/years, a user will accumulate many more objects than is currently present per user in the ORBIT dataset. Overall, however, training with a cap of 6 or more objects yields roughly equivalent performance to that reported in Table 5 where no caps are imposed during training. Since ORBIT test users have up to 12 objects (see Figure A.5c), our results suggest that a minimum of half the number of ultimate objects for a test user may be sufficient for meta-training. We repeat these analyses for the other metrics in Figures A.7 and A.8, and include the corresponding tables in Tables A.5 and A.6. We also investigate the impact of the number of tasks sampled per train user, included in Appendix G.

6. Discussion

We present the ORBIT dataset and benchmark, both grounded in the few-shot application of TORS for people who are blind/low-vision. Baseline performance and further analyses demonstrate, however, that current few-shot approaches struggle on realistic, high-variation data. This

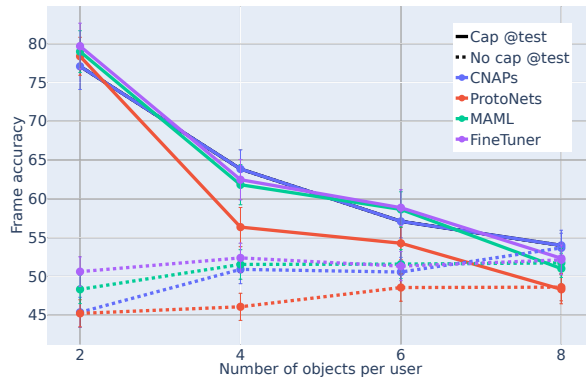


Figure 6: Meta-training and -testing with more objects per user poses a harder recognition problem (solid line), however meta-training with fewer objects than encountered at meta-testing (dashed line) shows only a small performance drop in CLU-VE compared to Table 5, suggesting that models may be able to adapt to more objects in the real-world.

gap offers opportunities for new and exciting research, from making models robust to high-variation data to quantifying the uncertainty in model predictions. More than just pushing the state-of-the-art in existing lines of thought, the ORBIT dataset opens up new types of challenges that derive from systems that will support human-AI partnership. We close by discussing three of these unique characteristics.

ORBIT’s user-centric formulation provides a unique opportunity to measure how well the ultimate system will work in the hands of real-world users. This contrasts most few-shot (and other) benchmarks which retain no notion of the end-user. Our results show that the baselines do not perform consistently across users. In the real-world, the heterogeneity of users, their objects, videoing techniques and devices will make this even more challenging. It will therefore be important for models to quantify, explain and ultimately minimize variation across users, particularly as models are deployed in a wider variety of scenarios outside the high-income countries in which the dataset was collected.

Directly involving users in the collection of a dataset intended to drive ML research does present some challenges. It can be difficult to reach the scale of web-scraped datasets [8, 28, 48] and users need an understanding of the potential system to contribute useful data. Building the system first would address this challenge, but it cannot be done without innovation of the algorithms. The ORBIT dataset is a starting point. It can be used to build the first generation of TORS which can be deployed and themselves then be used to collect more real-world data to develop a circle of innovation between dataset and application.

Finally, grounding in a real-world application encourages us, as researchers, to innovate in new directions to meet

the real-world conditions of deployment. This could range from new models and algorithms that are light enough to be personalized directly on a user’s phone to new research problems like handling the ‘no object’ scenario when none of a user’s objects are in the target scene.

In conclusion, the ORBIT dataset aims to shape the next generation of recognition tools for the blind/low-vision community, starting with TORS, and the robustness of vision systems across a broad range of other applications.

Acknowledgments

The ORBIT Dataset is funded by the Microsoft AI for Accessibility program. Luisa Zintgraf is supported by the 2017 Microsoft Research PhD Scholarship Program, and the 2020 Microsoft Research EMEA PhD Award. We thank VICTA, the Royal National College for the Blind (RNC), the Royal National Institute of Blind People (RNIB), the Canadian National Institute of Blind People (CNIB), Humanware, Tekvision School for the Blind, Blind South Africa (BlindSA), the National Federation of the Blind (NFB), and AbilityNet. We also thank Emily Madsen for helping with video validation. Finally, we thank all ORBIT collectors for their time and contributions.

References

- [1] Andrei Barbu, David Mayo, Julian Alverio, William Luo, Christopher Wang, Dan Gutfreund, Josh Tenenbaum, and Boris Katz. Objectnet: A large-scale bias-controlled dataset for pushing the limits of object recognition models. In *Advances in Neural Information Processing Systems (NeurIPS)*, 2019. 2
- [2] Luca Bertinetto, João F. Henriques, Philip H.S. Torr, and Andrea Vedaldi. Meta-learning with differentiable closed-form solvers. In *International Conference on Learning Representations (ICLR)*, 2019. 1, 6
- [3] Piotr Bojanowski, Edouard Grave, Armand Joulin, and Tomas Mikolov. Enriching word vectors with subword information. *Transactions of the Association for Computational Linguistics*, 5:135–146, 2017. 15
- [4] Da Chen, Yuefeng Chen, Yuhong Li, Feng Mao, Yuan He, and Hui Xue. Self-supervised learning for few-shot image classification. *arXiv preprint arXiv:1911.06045*, 2019. 1, 2
- [5] Yinbo Chen, Xiaolong Wang, Zhuang Liu, Huijuan Xu, and Trevor Darrell. A new meta-baseline for few-shot learning. *arXiv preprint arXiv:2003.04390*, 2020. 4, 5, 6, 7, 24, 26, 27, 28, 29
- [6] Mircea Cimpoi, Subhansu Maji, Iasonas Kokkinos, Sammy Mohamed, and Andrea Vedaldi. Describing textures in the wild. In *Conference on Computer Vision and Pattern Recognition (CVPR)*, 2014. 1, 2
- [7] Dima Damen, Hazel Doughty, Giovanni Maria Farinella, Sanja Fidler, Antonino Furnari, Evangelos Kazakos, Davide Moltisanti, Jonathan Munro, Toby Perrett, Will Price, and Michael Wray. Scaling Egocentric Vision: The EPIC-KITCHENS Dataset. In *European Conference on Computer Vision (ECCV)*, 2018. 2
- [8] Jia Deng, Wei Dong, Richard Socher, Li-Jia Li, Kai Li, and Li Fei-Fei. ImageNet: A large-scale hierarchical image database. In *Conference on Computer Vision and Pattern Recognition (CVPR)*, 2009. 2, 8
- [9] SM Ali Eslami, Danilo Jimenez Rezende, Frederic Besse, Fabio Viola, Ari S Morcos, Marta Garnelo, Avraham Ruderman, Andrei A Rusu, Ivo Danihelka, Karol Gregor, et al. Neural scene representation and rendering. *Science*, 360(6394):1204–1210, 2018. 3
- [10] Chelsea Finn, Pieter Abbeel, and Sergey Levine. Model-agnostic meta-learning for fast adaptation of deep networks. In *International Conference on Machine Learning (ICML)*, 2017. 1, 4, 5, 6, 7, 23, 24, 26, 27, 28, 29
- [11] Jonathan Gordon, John Bronskill, Matthias Bauer, Sebastian Nowozin, and Richard E. Turner. Meta-learning probabilistic inference for prediction. In *International Conference on Learning Representations (ICLR)*, 2019. 1, 4, 6
- [12] Raghav Goyal, Samira Ebrahimi Kahou, Vincent Michalski, Joanna Materzyńska, Susanne Westphal, Heuna Kim, Valentin Haenel, Ingo Freund, Peter Yianilos, Moritz Mueller-Freitag, et al. The “something something” video database for learning and evaluating visual common sense. In *International Conference on Computer Vision (ICCV)*, 2017. 2
- [13] Danna Gurari, Qing Li, Abigale J. Stangl, Anhong Guo, Chi Lin, Kristen Grauman, Jiebo Luo, and Jeffrey P. Bigham. VizWiz grand challenge: Answering visual questions from blind people. In *Conference on Computer Vision and Pattern Recognition (CVPR)*, 2018. 2
- [14] Kaiming He, Georgia Gkioxari, Piotr Dollár, and Ross Girshick. Mask r-cnn. In *International Conference on Computer Vision (ICCV)*, 2017. 1
- [15] Kaiming He, Xiangyu Zhang, Shaoqing Ren, and Jian Sun. Deep residual learning for image recognition. In *Conference on Computer Vision and Pattern Recognition (CVPR)*, 2016. 24
- [16] Yuqing Hu, Vincent Gripon, and Stéphane Pateux. Leveraging the feature distribution in transfer-based few-shot learning. *arXiv preprint arXiv:2006.03806*, 2020. 1, 2
- [17] Jonas Jongejan, Henry Rowley, Takashi Kawashima, Jongmin Kim, and Nick Fox-Gieg. The Quick, Draw! – A.I. experiment, 2016. 1, 2
- [18] Hernisa Kacorri. Teachable machines for accessibility. *ACM SIGACCESS Accessibility and Computing*, (119):10–18, 2017. 2, 3
- [19] Hernisa Kacorri, Utkarsh Dwivedi, Sravya Amancherla, Mayanka Jha, and Riya Chanduka. Includet: A data surfacing repository for accessibility datasets. In *The 22nd International ACM SIGACCESS Conference on Computers and Accessibility, ASSETS ’20*, New York, NY, USA, 2020. Association for Computing Machinery. 2
- [20] Hernisa Kacorri, Kris M. Kitani, Jeffrey P. Bigham, and Chieko Asakawa. People with visual impairment training personal object recognizers: Feasibility and challenges. In *ACM Conference on Human Factors in Computing Systems (CHI)*, 2017. 3

- [21] Diederik P. Kingma and Jimmy Ba. Adam: A method for stochastic optimization. *International Conference on Learning Representations (ICLR)*, 2015. 24, 25
- [22] Pang Wei Koh, Shiori Sagawa, Henrik Marklund, Sang Michael Xie, Marvin Zhang, Akshay Balsubramani, Weihua Hu, Michihiro Yasunaga, Richard Lanus Phillips, Sara Beery, et al. Wilds: A benchmark of in-the-wild distribution shifts. *arXiv preprint arXiv:2012.07421*, 2020. 2
- [23] Steinar Laenen and Luca Bertinetto. On episodes, prototypical networks, and few-shot learning. *arXiv preprint arXiv:2012.09831*, 2020. 5
- [24] Brenden Lake, Ruslan Salakhutdinov, Jason Gross, and Joshua Tenenbaum. One shot learning of simple visual concepts. In *Proceedings of the annual meeting of the cognitive science society*, volume 33, 2011. 1, 2, 3
- [25] Kyungjun Lee and Hernisa Kacorri. Hands holding clues for object recognition in teachable machines. In *ACM Conference on Human Factors in Computing Systems (CHI)*, pages 1–12, 2019. 2, 3
- [26] Yong Jae Lee, Jaechul Kim, and Kristen Grauman. Key-segments for video object segmentation. In *2011 International conference on computer vision*, pages 1995–2002. IEEE, 2011. 4
- [27] Xiaomeng Li, Lequan Yu, Yueming Jin, Chi-Wing Fu, Lei Xing, and Pheng-Ann Heng. Difficulty-aware meta-learning for rare disease diagnosis. In *International Conference on Medical Image Computing and Computer-Assisted Intervention*, pages 357–366. Springer, 2020. 3
- [28] Tsung-Yi Lin, Michael Maire, Serge Belongie, James Hays, Pietro Perona, Deva Ramanan, Piotr Dollár, and C. Lawrence Zitnick. Microsoft COCO: Common Objects in Context. In *European Conference on Computer Vision (ECCV)*, 2014. 1, 2, 8
- [29] Vincenzo Lomonaco and Davide Maltoni. Core50: a new dataset and benchmark for continuous object recognition. In Sergey Levine, Vincent Vanhoucke, and Ken Goldberg, editors, *Proceedings of the 1st Annual Conference on Robot Learning*, volume 78 of *Proceedings of Machine Learning Research*, pages 17–26. PMLR, 13–15 Nov 2017. 2, 4
- [30] Vincenzo Lomonaco, Davide Maltoni, and Lorenzo Pellegrini. Rehearsal-free continual learning over small non-iid batches. In *2020 IEEE/CVF Conference on Computer Vision and Pattern Recognition Workshops (CVPRW)*, pages 989–998. IEEE Computer Society, 2020. 4
- [31] Xiankai Lu, Wenguan Wang, Jianbing Shen, Yu-Wing Tai, David J Crandall, and Steven CH Hoi. Learning video object segmentation from unlabeled videos. In *Proceedings of the IEEE/CVF conference on computer vision and pattern recognition*, pages 8960–8970, 2020. 4
- [32] Dhruv Mahajan, Ross Girshick, Vignesh Ramanathan, Kaiming He, Manohar Paluri, Yixuan Li, Ashwin Bharambe, and Laurens van der Maaten. Exploring the limits of weakly supervised pretraining. In *European Conference on Computer Vision (ECCV)*, 2018. 1
- [33] Maria-Elena Nilsback and Andrew Zisserman. Automated flower classification over a large number of classes. In *Indian Conference on Computer Vision, Graphics & Image Processing (ICVGIP)*, 2008. 1, 2
- [34] Eunbyung Park and Junier B Oliva. Meta-curvature. *arXiv preprint arXiv:1902.03356*, 2019. 1, 2
- [35] Federico Perazzi, Anna Khoreva, Rodrigo Benenson, Bernt Schiele, and Alexander Sorkine-Hornung. Learning video object segmentation from static images. In *Proceedings of the IEEE conference on computer vision and pattern recognition*, pages 2663–2672, 2017. 4
- [36] Ethan Perez, Florian Strub, Harm De Vries, Vincent Dumoulin, and Aaron Courville. FiLM: Visual reasoning with a general conditioning layer. In *Association for the Advancement of Artificial Intelligence (NAACL)*, 2018. 24
- [37] Joseph Redmon and Ali Farhadi. Yolo9000: better, faster, stronger. In *Conference on Computer Vision and Pattern Recognition (CVPR)*, 2017. 1
- [38] Shaoqing Ren, Kaiming He, Ross Girshick, and Jian Sun. Faster r-cnn: Towards real-time object detection with region proposal networks. In *Advances in Neural Information Processing Systems (NeurIPS)*, 2015. 1
- [39] James Requeima, Jonathan Gordon, John Bronskill, Sebastian Nowozin, and Richard E. Turner. Fast and flexible multi-task classification using conditional neural adaptive processes, 2019. 1, 4, 5, 6, 7, 23, 24, 26, 27, 28, 29
- [40] Olga Russakovsky, Jia Deng, Hao Su, Jonathan Krause, Sanjeev Satheesh, Sean Ma, Zhiheng Huang, Andrej Karpathy, Aditya Khosla, Michael Bernstein, Alexander C. Berg, and Li Fei-Fei. ImageNet Large Scale Visual Recognition Challenge. *International Journal of Computer Vision (IJCV)*, 115(3):211–252, 2015. 1, 2, 24
- [41] Jake Snell, Kevin Swersky, and Richard Zemel. Prototypical networks for few-shot learning. In *Advances in Neural Information Processing Systems (NeurIPS)*, 2017. 1, 4, 5, 6, 7, 23, 24, 26, 27, 28, 29
- [42] Joan Sosa-García and Francesca Odone. “Hands on” visual recognition for visually impaired users. *ACM Transactions on Accessible Computing (TACCESS)*, 10(3):1–30, 2017. 2
- [43] Christian Szegedy, Sergey Ioffe, Vincent Vanhoucke, and Alexander A. Alemi. Inception-v4, inception-resnet and the impact of residual connections on learning. In *Association for the Advancement of Artificial Intelligence (NAACL)*, 2017. 1
- [44] Mingxing Tan and Quoc Le. Efficientnet: Rethinking model scaling for convolutional neural networks. In *International Conference on Learning Representations (ICLR)*, 2019. 1
- [45] Sebastian Thrun and Lorien Pratt. *Learning to learn*. Springer Science & Business Media, 2012. 1
- [46] Yonglong Tian, Yue Wang, Dilip Krishnan, Joshua B Tenenbaum, and Phillip Isola. Rethinking few-shot image classification: a good embedding is all you need? *arXiv preprint arXiv:2003.11539*, 2020. 1, 4, 5, 6, 7, 24, 26, 27, 28, 29
- [47] Hugo Touvron, Andrea Vedaldi, Matthijs Douze, and Hervé Jégou. Fixing the train-test resolution discrepancy: Fixefficientnet. *arXiv preprint arXiv:2003.08237*, 2020. 1
- [48] Eleni Triantafillou, Tyler Zhu, Vincent Dumoulin, Pascal Lamblin, Kelvin Xu, Ross Goroshin, Carles Gelada, Kevin Swersky, Pierre-Antoine Manzagol, and Hugo Larochelle. Meta-dataset: A dataset of datasets for learning to learn from few examples. *arXiv preprint arXiv:1903.03096*, 2019. 1, 2, 3, 7, 8, 24

- [49] Oriol Vinyals, Charles Blundell, Timothy Lillicrap, Daan Wierstra, et al. Matching networks for one shot learning. In *Advances in Neural Information Processing Systems (NeurIPS)*, 2016. 1, 2, 3, 4, 5, 6, 23
- [50] Catherine Wah, Steve Branson, Peter Welinder, Pietro Perona, and Serge Belongie. The Caltech-UCSD Birds-200-2011 dataset. Technical Report CNS-TR-2011-001, 2011. 1, 2
- [51] Jason Yosinski, Jeff Clune, Yoshua Bengio, and Hod Lipson. How transferable are features in deep neural networks? In *Advances in neural information processing systems*, pages 3320–3328, 2014. 6, 24
- [52] Egor Zakharov, Aliaksandra Shysheya, Egor Burkov, and Victor Lempitsky. Few-shot adversarial learning of realistic neural talking head models. In *International Conference on Computer Vision (ICCV)*, 2019. 3
- [53] Amy Zhao, Guha Balakrishnan, Fredo Durand, John V Guttag, and Adrian V Dalca. Data augmentation using learned transformations for one-shot medical image segmentation. In *Conference on Computer Vision and Pattern Recognition (CVPR)*, 2019. 3
- [54] Luisa M. Zintgraf, Kyriacos Shiarlis, Vitaly Kurin, Katja Hofmann, and Shimon Whiteson. Fast context adaptation via meta-learning. In *International Conference on Machine Learning (ICML)*, 2019. 1, 6, 23

A. Unfiltered ORBIT dataset

A.1. Dataset collection protocol

The unfiltered ORBIT dataset was collected in two phases, the first with blind/low-vision collectors based only in the UK, and the second with blind/low-vision collectors globally. Collectors were recruited via blind charities and networks, and were screened for blindness/low-vision before beginning the collection task. Following this, they were sent instructions for collecting the videos using an accessible iOS app (see [Appendix A.2](#)).

A.1.1 Phase 1 protocol

Collectors were asked to record videos for at least 10 objects, including at least 2 large or immovable objects. For each of these objects, they were asked to record two types of videos, ‘train’ and ‘test’ which correspond to ‘clean’ and ‘clutter’, respectively. Collectors were asked to adopt specific video recording techniques to help capture their objects in-frame.

For clean videos, the collector was asked to place the object on a clear surface with no other objects present and record a video of the object, repeating this on at least 6 different surfaces. Collectors were given step-by-step instructions to record these using a ‘zoom-out’ technique:

1. Keep one hand on the surface next to the object as an anchor point to help aim the camera at the object
2. Hold the phone in your other hand and bring it as close as possible to the object
3. Start recording, then slowly draw the phone away from the object until it reaches your body at shoulder height
4. Rotate the object so that a different side is facing you, while returning the phone to your anchor hand
5. Repeat this at least 3 times for different sides of the object, then stop recording

We helped collectors time each rotation by playing a tick sound every 5 seconds, and asking them to record a new side of the object between ticks. To prevent inadvertently long videos, we automatically ended recordings after 2 minutes.

For large or immovable objects, collectors were asked to position themselves relative to the object so that they were recording different aspects or angles of the object. Again, they were asked to place an ‘anchor hand’ on three different parts or positions of the object, and then draw their phone slowly towards their body. We asked them to record the object from 3 different angles, repeated this twice, to provide a total of clean videos.

For clutter videos, collectors were asked to construct a cluttered ‘scene’ based on a real-life situation in which the recognizer might be used, for example, a surface on which an object may have been moved. The scene needed to include at least 5 other ‘distractor objects’ that did not include any of the user’s selected objects. For immovable objects like

a front door, we asked them to position some likely objects around or in front of it, such as packages, umbrellas, or shoes. Collectors were asked to record their clutter videos using 2 different techniques: a ‘zoom-out’ and a ‘panning’ technique, recording at least one video of each technique for each of their objects. For the ‘zoom-out’ technique, similar to the clean videos, they were asked to place an ‘anchor hand’ in the scene, and then draw their phone slowly towards their body, before ending the recording. For the ‘panning’ technique, collectors were asked to place an anchor hand in the scene, making sure the selected object was not directly in front of them, and . They were then asked to remove their anchor hand, and pan over the scene at shoulder height from right to left, by turning their upper body.

A.1.2 Phase 2 protocol

In Phase 2, we reduced the number of objects to at least 5 per collector, with no specification for large or immovable objects. We also reduced the number of videos to 5 clean (taken on 5 different surfaces) and 2 clutter videos. For clean videos, collectors were asked to use the ‘zoom-rotate’ technique, showing four sides of the object. For clutter videos, instead of creating a real-world scene as in Phase 1, collectors were asked to record the object, including its surroundings, in a scene where it would normally be found. For simplicity, the panning technique was dropped, and collectors were asked to record both clutter videos using the ‘zoom-out’ technique. For the second clutter video, they were simply asked to record it from a different position. Finally, we reduced the cut-off video time to 30 and 20 seconds for clean and clutter videos respectively.

A.2. ORBIT Camera iOS app

The dataset was collected using a custom-built iOS app (see [Figure A.1](#)) that followed Apple’s accessibility guidelines and was tested with blind/low-vision users. With the app, collectors could add a new object by entering the object’s name into a text box on the home screen. This name served as the label for all that object’s videos. The collector could then navigate to a second screen to i) record new videos, and ii) review videos already recorded for that object. Here, the collector could also delete and re-record videos already stored. Status indicators were available for each recorded video, including whether it was uploaded to the data server, validated, and visible in the public dataset.

All contributed videos were uploaded to a data server which provided administrative functionality. Administrators were able to set-up data collection periods, review videos uploaded by collectors, and mark them as reviewed and safe for export. All videos were manually checked to ensure i) the labeled object was present in the video, ii) the video did not contain any personally identifiable information (PII), and

iii) the object as well as object name were appropriate. If a video did not meet all of these criteria, it was removed from the server, and the collector received a notification via the app to re-record the video. All PII obtained via the consent screen was encrypted, and decryption keys were held by administrators outside the server.

Code for the app and back-end data server is open-sourced at <https://github.com/orbit-a11y>.



Figure A.1: ORBIT Camera iOS app: (left) Informed consent screen, (center-left) the ‘Things’ screen shows a user’s library of personal objects, (center-right) a ‘Thing’ screen for a specific object, (right) a ‘Thing’ screen after recording a video

A.3. Unfiltered dataset summary

The unfiltered ORBIT dataset contains 4733 videos (3,161,718 frames, 97GB) of 588 objects, collected by 97 people who are blind/low-vision. We summarize it in [Table A.1](#) and describe it in more detail below.

Number of collectors 97 blind/low-vision collectors contributed to the unfiltered ORBIT dataset.

Numbers of videos and objects Collectors contributed a total of 588 objects and 4,733 videos. 3,356 of these videos showed the object in isolation, referred to as *clean* videos, while 1,377 showed the object in realistic, multi-object scenes, referred to as *clutter* videos. Of the clutter videos, 873 were recorded with the zoom-rotate technique, and 504 with the panning technique (see video techniques in [Appendix A.1](#)). Each collector contributed on average 6.1 (± 3.8) objects, with 34.6 (± 41.5) clean videos, 9.0 (± 10.5) clutter-zoom-out videos, and 5.2 (± 10.5) clutter-pan videos per object. [Figure A.2](#) shows the number of objects ([A.2a](#)) and number of videos per collector ([A.2b](#)).

Types of objects We group these objects into clusters based on object similarity, and show their long-tailed distribution in [Figure A.6a](#). The clustering algorithm and full contents of each cluster are included in [Appendix D](#).

B. ORBIT benchmark dataset preparation

The ORBIT benchmark dataset is a subset of the unfiltered ORBIT dataset, and is selected to meet the requirements of the ORBIT benchmark ([Section 4](#)). The following sections detail the steps to prepare the benchmark dataset.

B.1. File structure

The following summarizes the file hierarchy of the ORBIT benchmark dataset:

```
> mode (train/validation/test)
> user  $\kappa$ 
  > object  $p \in \mathcal{P}^\kappa$ 
    > clean
      > video  $\bar{v}_i \in \bar{\mathcal{V}}_p^\kappa$ 
        · frame  $v_1$ 
        · ...
        · frame  $v_{F_i}$ 
    > clutter
      > video  $v_i \in \mathcal{V}_p^\kappa$ 
```

B.2. Video filtering

From the 97 collectors who submitted 4,733 videos (3,356 clean, 873 clutter, 504 clutter-pan) in the unfiltered dataset, the videos of 77 collectors were selected for the benchmark dataset — a total of 3,822 videos (2,996 clean, 826 clutter, 0 clutter-pan) of 486 objects (see [Table 2](#) and [Figure 2](#)). The following steps detail the video selection procedure:

1. All clutter-pan videos were removed (504 videos, 4 objects, 0 collectors). This was done to maintain consistency because the panning technique was explored in the first, but not the second, phase of the dataset collection. Clutter-zoom-out videos are therefore referred to as simply clutter videos in the benchmark dataset.
2. Videos shorter than 1 second were removed (20 videos, 0 objects, 0 collectors). Extremely short videos were assumed to be a mistaken recording.
3. Objects with < 2 clean videos and < 1 clutter video were removed (387 videos, 101 objects, 20 collectors). These were the minimum numbers required for the benchmark evaluation.

B.3. Train/validation/test sets

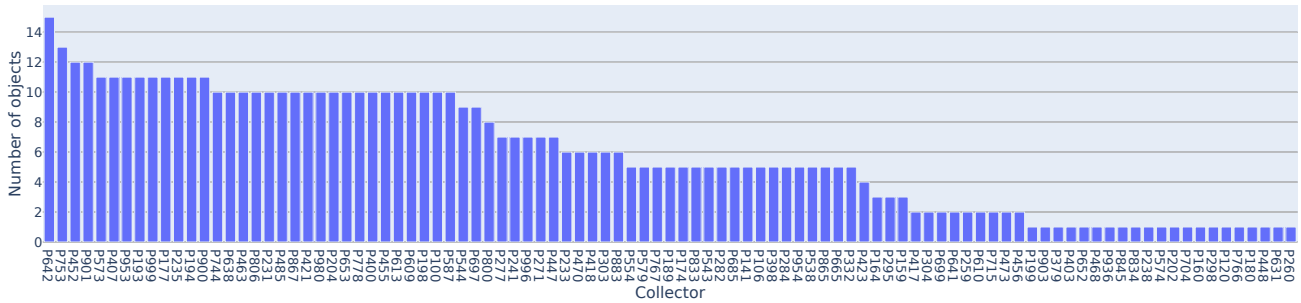
Of the 77 collectors remaining, 12 contributed only 1 object. To avoid discarding these videos, we merged these collectors together (or with others who had only contributed 2 objects) to enforce a minimum of 3 objects per collector³. This yielded an effective total of 67 benchmark users. These 67 users were then split into train/validation/test users (44/6/17, respectively)⁴, according to the following criteria:

³See merged collectors in `data/orbit_benchmark_users_to_split.json` in the repository

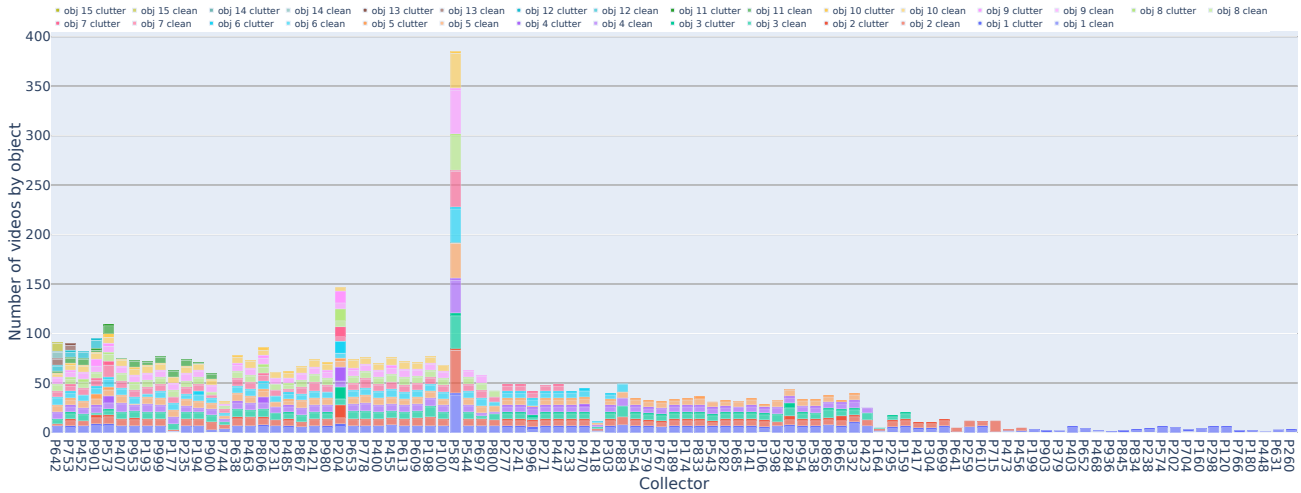
⁴See `data/orbit_benchmark_mode_splits.json` in the repository

	Collectors	Objects	Videos	Videos per object			Frames per video		
				mean/std	25/75 th perc.	min/max	mean/std	25/75 th perc.	min/max
Total	97	588	4733	8.0/5.5	7.0/8.0	1.0/49.0	668.0/411.1	355.0/898.0	2.0/3600.0
Clean		576	3356	5.8/4.4	5.0/6.0	1.0/44.0	763.0/416.7	504.0/900.0	2.0/3600.0
Clutter-zoom-out		519	873	1.7/1.4	1.0/2.0	1.0/14.0	452.3/270.7	241.0/598.0	3.0/3596.0
Clutter-pan		330	504	1.5/1.6	1.0/1.0	1.0/12.0	408.9/310.4	186.0/521.0	8.0/2684.0
Per-collector	1	6.1/3.8	48.8/53.7	6.7/4.5	5.0/7.7	1.0/41.5	667.2/222.2	550.6/808.4	73.0/1467.2
Clean		6.1/3.8	35.1/41.2	5.0/3.6	4.0/6.0	1.0/36.6	774.9/287.1	648.9/898.7	134.5/1872.6
Clutter-zoom-out		6.0/3.8	10.3/10.6	1.8/1.4	1.0/2.0	1.0/12.0	465.1/191.8	329.2/597.1	73.0/1258.8
Clutter-pan		6.1/3.8	9.8/11.4	1.6/1.6	1.0/1.4	1.0/8.6	419.5/231.4	239.0/574.3	164.5/1208.4

Table A.1: Unfiltered ORBIT dataset



(a) Number of objects per collector



(b) Number of videos (stacked by object) per collector

Figure A.2: Number of objects and videos across 97 collectors in the unfiltered ORBIT dataset

Validation/test user criteria We enforced that validation and test users should have at least 5 objects to ensure the test case was sufficiently challenging. In total, 53 out of 67 users met this criteria, from which we randomly sampled 17 test users and 6 validation users.

Train user criteria The remaining 44 users were marked as train users (14 of which did not meet the above criteria).

B.4. Video pre-processing

Videos were split into frames using `ffmpeg` at a rate of 30 FPS. Frames were also re-sized from 1080×1080 pixels to 84×84 . This was primarily done for GPU memory purposes, and future work will involve scaling the pipeline to larger images.

C. Extended benchmark dataset summary

In Section 3, we summarize the benchmark dataset over all 67 users. Here, we report the same summaries but now grouped by train/validation/test users. First, mirroring Table 2, we report the statistics for train/validation/test users in Table A.2. We include the object cluster histogram for all benchmark users in Figure A.6b, and for train (A.6c), validation (A.6d) and test (A.6e) users. Finally, extending Figure 1, we include more examples of clean and clutter frames from the ORBIT benchmark dataset in Figure A.3.

D. Object clustering

The objects submitted by collectors varied widely in high-level object categories. To quantify this variation, we grouped objects into clusters based on object similarity.

Clustering algorithm Each object label (as entered by the user in the app) was converted to lowercase, tokenized and parts-of-speech tagged (using NLTK). A weighted average of all nouns (NN, NNS) in the label was computed (each represented as a FastText [3] embedding)⁵ where each weight was the (normalized) frequency of the noun across all nouns in the dataset. Intuitively, this encouraged more common nouns to dominate the object label’s embedding (and down-weighted typos and collectors’ idiosyncrasies). We then clustered these embeddings using an agglomerative clustering algorithm based on pair-wise cosine distances⁶. This produced cluster proposals which we then manually tweaked to obtain the final clusterings shown in Figure A.6

Clusters for Figure A.6a [97 users, 588 objects, 132 clusters] 1: keys, house keys, radar key, my keys, front door keys, keychain, door keys, key, set of keys, 2: remote, tv remote, apple tv remote, amazon remote control, television remote control, remote control, virgin remote control, tv remote control, samsung tv remote control, presentation remote, sky q remote, clickr, fire stick remote, control, television control, remote tv, remote control, apple tv ii remote control, t. v. remote control, 3: black small wallet, my purse, my wallet, ladies purse, money pouch, coin purse, wallet for bus pass cards and money, i d wallet, ipod in wallet, wallet, wallet, purse, 4: symbol cane, black mobility cane, my cane, white mobility cane, folded white cane, long cane, cane, folded cane, folded long guide cane, p939411 white cane, white cane, visibility stick, mobility, mobility cane, white cane, 5: earphones, apple headphones, apple earpods, airpods, my airpod pros case, iphone air pods, airpods pro charging case, airpod case, airpods, my airpods, airpods case, earpods, apple airpods case, 6: mug, personal mug,

cup again, coffee mug, toddler cup, styrofoam cup, my mug, my cup, 7: front door, back door, house door, front door to house, door, my front door, shed door, front door from outside, 8: blue headphones, my headphones, headphone, bose wireless headphones, headset, my sennheiser pxc 350-2, headphones, 9: phone, mobile phone, iphone 6, apple mobile phone, i phone 11 pro, iphone in case, iphone, cell phone, work phone, phone case, 10: watch, wrist watch, apple watch, apple watch, risk watch, my apple watch, 11: backpack, my work backpack, work bag, bag, shoulder bag, bum bag, back pack, work backpack, sports bag, sport bago, numb bag, 12: sunglasses, my wraparound sunglasses, dark glasses, 13: slippers, nike trainers, my shoes, boot, trainers, trainer shoe, slipper, my trainers, shoes, running shoes, 14: medication, blister pack of painkillers, tablets, money, aspirin vs tylenol, aspirin, pill bottle, my pill dosette, buckleys, box of tablets, 15: victor stream book reader, orbit braille reader and notetaker, victor reader stream, orbit reader 20 braille display, braillepen slim braille keyboard, braille orbit reader, solo audiobook player, braille note, my braille display, rnib talking book envelope, 16: guide dog play cola, dogs lead, guide dog harness, retractable dog lead, leash, guide dog harness, dog lead, dogs, running tether, 17: blue tooth keyboard, bluetooth keyboard, my keyboard, apple wireless keyboard, mini bluetooth keyboard, portable keyboard, keyboard, 18: my water bottle, bottle, pop bottle, green water bottle, water bottle, bottle of water, clean canteen stainless steel water bottle, 19: reading glasses, glasses, eye glasses, spectacles, 20: adaptive washing machine, washing machine, tumble dryer, adaptive dryer, tumble dry setting washing machine, washing machine setting, 21: baseball cap, cap, orange skullcap, my tilly hat, hat, my tilly hat upside down, 22: microwave, toaster, kettle, one cup kettle, 23: digital dab radio, dab radio, speaker, radio, my bose bluetooth speaker, 24: wheely bin, wheelie bin, black bin, recycling bin, bin, brown wheelie bin, 25: hairbrush, comb, hair brush, 26: necklace, brown leather bracelet, ladies silver bracelet, favourite earrings, silver male wedding band, clear quartz, 27: screwdriver, small space screwdriver, small screwdriver, spanner, wood phillips head, pex plumbers pliers, wood screw phillips head, 28: 12 measuring cup, 13 measuring cup, 14 measuring cup, 1 cup measuring cup, measuring spoon, measuring spoons, 29: lime green marker, yellow marker, pink marker, magenta marker, reptile green marker, pen, 30: digital recorder, dictaphone, pen friend, handheld police scanner, 31: face mask, covid mask, my purple mask, blue facemask, 32: airpod pro, single airpod, apple airpods, pro, 33: wireless earphones, bone conducting headset, bose earpods, my muse s headband, 34: phone stand, mobile phone stand, ipod stand, iphone stand, 35: memory stick, usb c dongle, usb stick, usb, 36: apple phone charger, phone charger, 37: scissors, secateurs, 38: car, my sisters car, 39: socks, sock, 40: fridge, fridge freezer indicator, 41: tv unit, flat screen television, tv,

⁵If the label had no nouns or only 1 word, the whole label was kept.

⁶With a distance threshold of 0.4.

	Users	Objects	Videos	Videos per object			Frames per video		
				mean/std	25/75 th perc.	min/max	mean/std	25/75 th perc.	min/max
Total	44	278	2277	8.2/6.0	7.0/7.0	3.0/46.0	716.8/448.6	378.0/898.0	34.0/3600.0
Clean			1814	6.5/6.0	5.0/6.0	2.0/44.0	774.0/471.6	394.5/899.0	34.0/3600.0
Clutter			463	1.7/0.8	1.0/2.0	1.0/7.0	492.7/235.5	324.5/599.0	47.0/2412.0
Per-user	1	6.3/2.6	51.8/55.2	7.6/4.8	6.5/7.4	3.4/38.4	735.5/232.0	629.7/805.7	213.1/1614.3
Clean			41.2/52.7	5.9/4.8	4.6/6.0	2.4/36.5	823.0/279.0	710.2/898.4	219.3/1872.6
Clutter			10.5/5.2	1.7/0.5	1.2/2.0	1.0/3.0	467.3/163.2	362.4/597.0	177.7/853.0

(a) Train users

	Users	Objects	Videos	Videos per object			Frames per video		
				mean/std	25/75 th perc.	min/max	mean/std	25/75 th perc.	min/max
Total	6	50	347	6.9/1.0	7.0/7.0	4.0/10.0	638.4/227.6	561.0/775.5	33.0/2053.0
Clean			284	5.7/1.0	5.0/6.0	3.0/9.0	689.6/210.3	626.0/835.0	33.0/2053.0
Clutter			63	1.3/0.6	1.0/1.0	1.0/4.0	407.7/144.1	289.0/593.5	176.0/618.0
Per-user	1	8.3/2.4	57.8/17.7	6.9/0.3	6.7/7.0	6.6/7.6	666.7/95.8	621.0/741.7	529.8/808.4
Clean			47.3/17.5	5.5/0.7	5.0/5.7	4.6/6.6	730.5/114.1	673.9/819.0	565.0/899.9
Clutter			10.5/0.8	1.4/0.4	1.0/1.8	1.0/2.0	409.8/133.2	313.3/528.4	250.5/597.9

(b) Validation users

	Users	Objects	Videos	Videos per object			Frames per video		
				mean/std	25/75 th perc.	min/max	mean/std	25/75 th perc.	min/max
Total	17	158	1198	7.6/2.4	7.0/7.0	3.0/19.0	696.4/384.8	428.0/900.0	40.0/3596.0
Clean			898	5.7/1.0	5.0/6.0	2.0/10.0	791.6/352.7	621.0/926.0	51.0/3596.0
Clutter			300	1.9/2.3	1.0/2.0	1.0/13.0	411.5/332.5	175.0/598.0	40.0/3596.0
Per-user	1	9.3/2.1	70.5/24.2	7.6/2.1	6.8/7.4	6.2/15.6	733.2/166.6	599.4/811.2	335.7/977.0
Clean			52.8/14.5	5.6/0.6	5.0/6.0	4.4/6.7	804.1/164.7	658.8/899.0	518.1/1095.6
Clutter			17.6/18.7	1.9/2.0	1.0/1.9	1.0/9.9	478.3/285.4	282.3/598.2	158.6/1258.8

(c) Test users

Table A.2: The ORBIT benchmark dataset grouped by train, validation and test users

smarttv, television, 42: prosecco, jd whisky bottle, bottle of alcoholic drink, vagabond ale bottle, 43: lighter, vape pen, cannabis vape battery, 44: pepper shaker, pink himalayan salt, mediterranean sea salt, salt grinder, 45: sunglasses case, glasses case, eyewear case, 46: lipstick, chap stick, lip balm, 47: tweezers, finger nail clipper, hook, 48: inhaler, insulin pen, spacer, 49: dining table setup, desk, garden table, 50: liquid level indicator, water level sensor, 51: bottle opener, corkscrew, 52: pint glass, wine glass, glass, 53: guide dog, my flea, 54: dog streetball, dog toy, adaptive tennis ball, 55: stylus, apple pencil, 56: my laptop, laptop, 57: ipad, ipad pro, 58: mouse, 59: local post box, post box, 60: black strappy vest, t-shirts, 61: gloves, winter gloves, 62: hand gel, lotion bottle, 63: perfume, deodorant, 64: hair clip, headband, 65: toothbrush, electric toothbrush, 66: alcohol wipe, skip prep, 67: my hearing aid, hearing aid, 68: magnifier, pocket magnifying glass, 69: blue artificial eye, green artificial eye, 70: hand saw, 71: tape measure, ruler, 72: electric sanding disc, miter saw, 73: valve oil, slide grease, 74: cooker, 75: shelf unit with things, wardrobe, 76: knitting basket, washing basket, basket, 77: home phone, cordless phone, 78: skipping

rope, spinner, 79: stairgate, back patio gate, 80: large sewing needle, knitting needle, 81: mayonnaise jar, mustard, 82: rice, chicken instant noodles, 83: tea, cranberry cream tea, 84: ottawa bus stop, bus stop sign, 85: journal, book, 86: security fob, 87: money clip, 88: headphone case, 89: ps4 controller, 90: compact disc, 91: garden wall, 92: garden shed, 93: litter and dog waste bin, 94: my clock, 95: sleep mask, 96: glasses cleaning wipe, 97: tissue box, 98: condom box, 99: make up, 100: clear nail varnish, 101: eye drops, 102: battery drill, 103: bed, 104: sofa, 105: cushion, 106: garden bench, 107: mirror, 108: table fan, 109: tred mill, 110: exercise bench, 111: watering can, watering, 112: vase with flowers, 113: veg peeler, 114: sharp knife, 115: wall plug, 116: embroidery thread cone, 117: hole punch, 118: pencil case, 119: paperclips, 120: uno cards, 121: baked bean tin, 122: banana, 123: cappuccino pods, 124: mountain dew can, 125: pinesol cleaner, 126: fish food, 127: cat, 128: dog poo, 129: my slate, 130: av tambourine, 131: grinder, 132: fluffy blanket

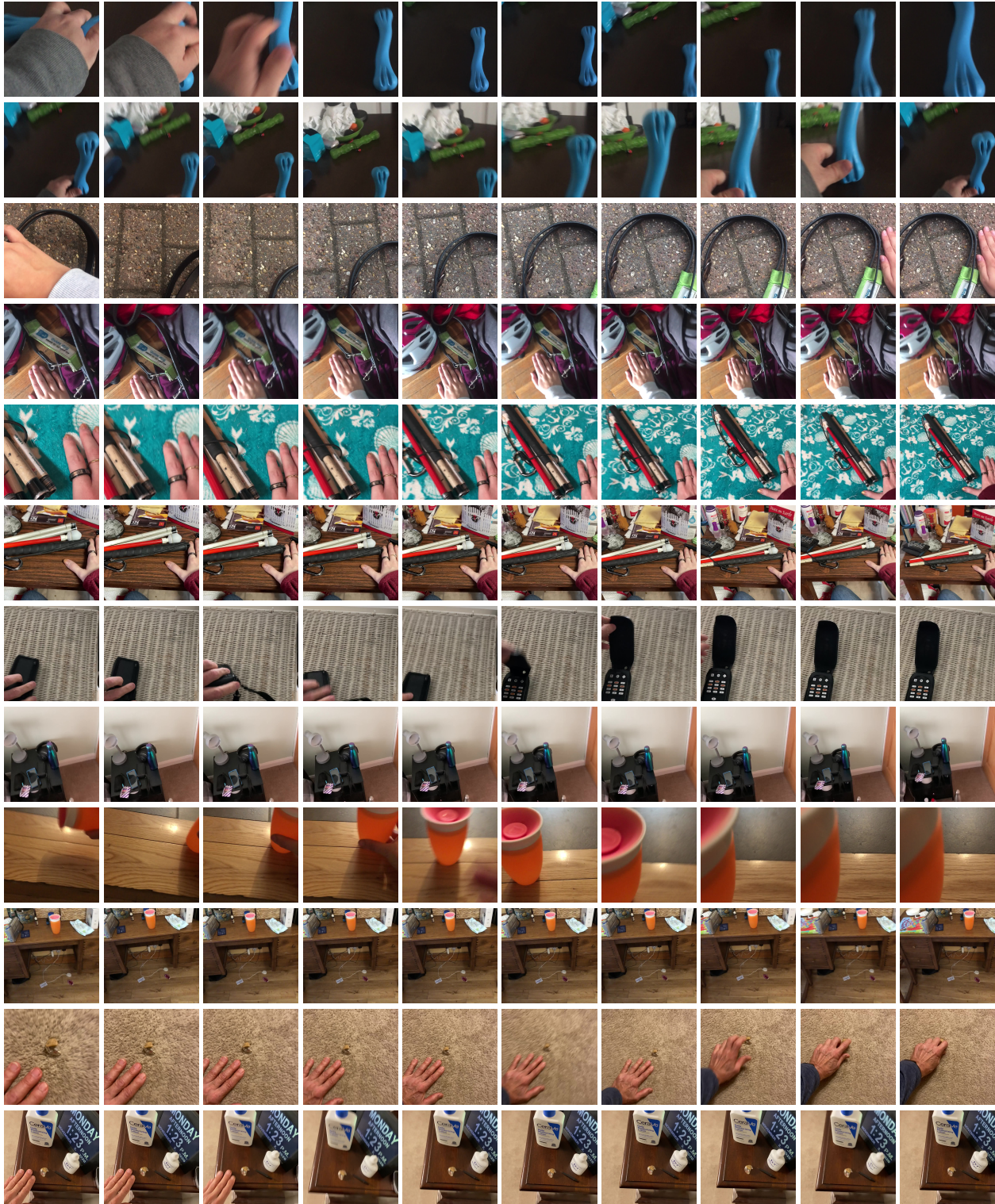
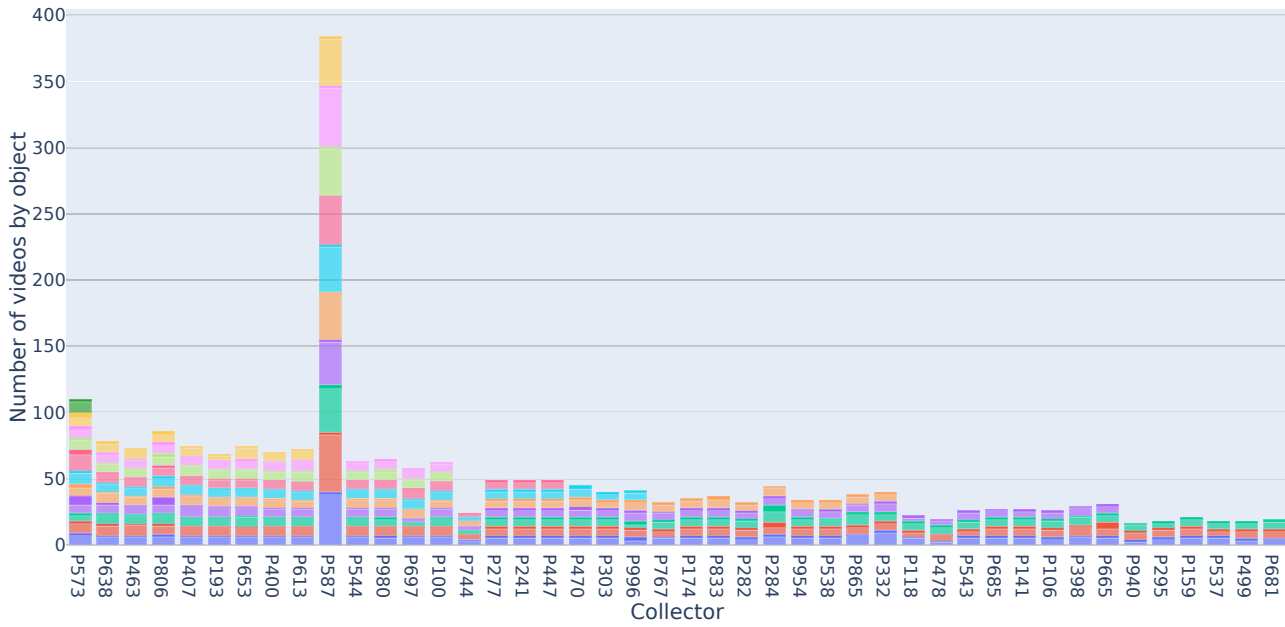
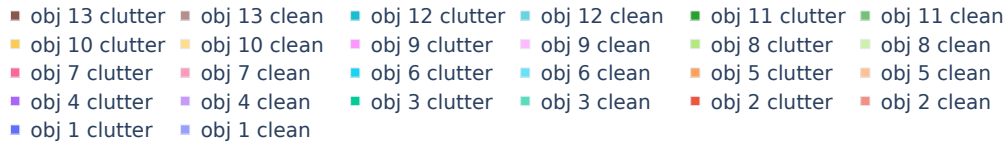
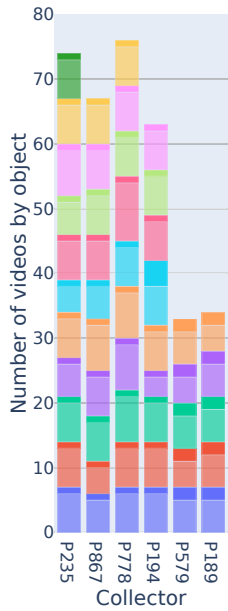


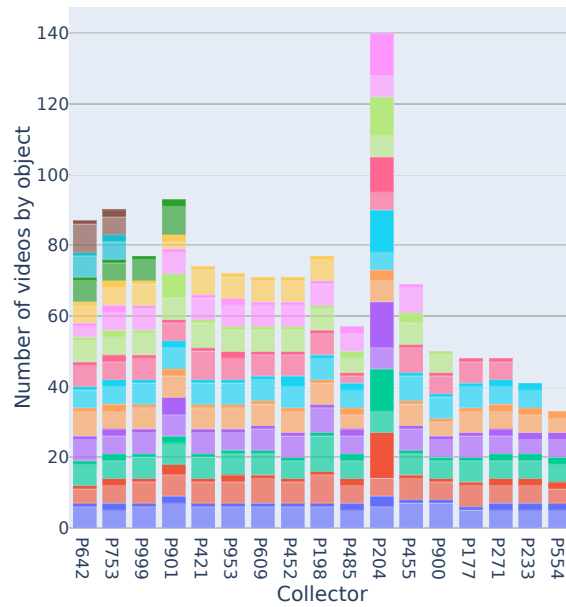
Figure A.3: Video clips from the ORBIT benchmark dataset. Each row comes from a different video (alternating clean and clutter). Rows 1,2: “dog toy”. Rows 3,4: “dog lead”. Rows 5,6: “white cane”. Rows 7,8: “victor stream book reader”. Rows 9,10: “toddler cup”. Rows 11,12: “hearing aid”.



(a) Train users



(b) Validation users

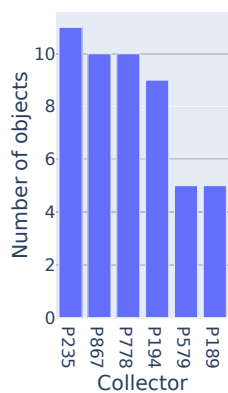


(c) Test users

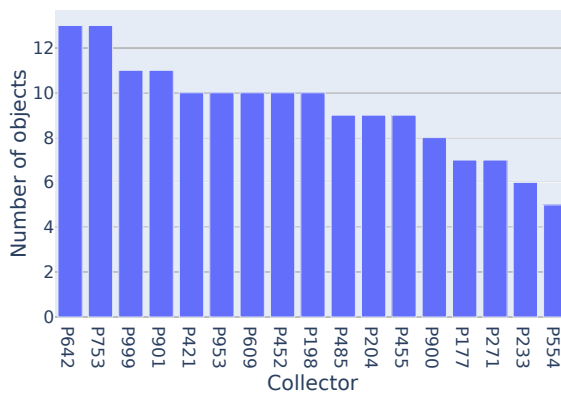
Figure A.4: Number of clean and clutter videos (stacked by object) per collector in the ORBIT benchmark dataset



(a) Train users



(b) Validation users

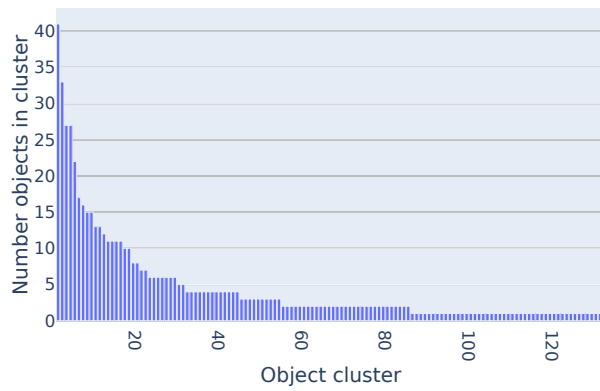


(c) Test users

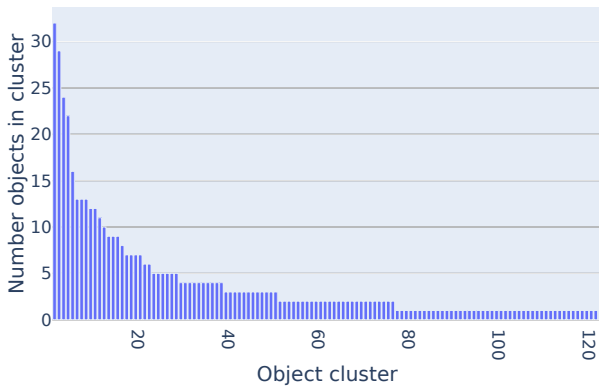
Figure A.5: Number of objects per collector in the ORBIT benchmark dataset

Clusters for Figure A.6b [67 users, 486 objects, 122 clusters] 1: keys, house keys, radar key, my keys, front door keys, keychain, door keys, key, set of keys, 2: remote, tv remote, apple tv remote, amazon remote control, television remote control, remote control, virgin remote control, tv remote control, samsung tv remote control, presentation remote, sky q remote, clickr, fire stick remote, control, television control, remote tv, 3: black small wallet, my purse, my wallet, ladies purse, money pouch, coin purse, wallet for bus pass cards and money, i d wallet, ipod in wallet, walletv, wallet, purse, 4: symbol cane, black mobility cane, my cane, white mobility cane, folded white cane, long cane, cane, folded cane, folded long guide cane, p939411 white cane, white came, visibility stick, mobility, mobility cane, white cane, 5: earphones, apple headphones, apple earpods, airpods, my airpod pros case, iphone air pods, airpods pro charging case, airpod case, airpods, my airpods, airpods case, earpods, 6: blue headphones, my headphones, headphone, bose wireless headphones, headset, my sennheiser pxc 350-2, headphones, 7: phone, mobile phone, iphone 6, apple mobile phone, i phone 11 pro, iphone in case, iphone, cell phone, work phone, phone case, 8: mug, personal mug, cup again, coffee mug, toddler cup, styrofoam

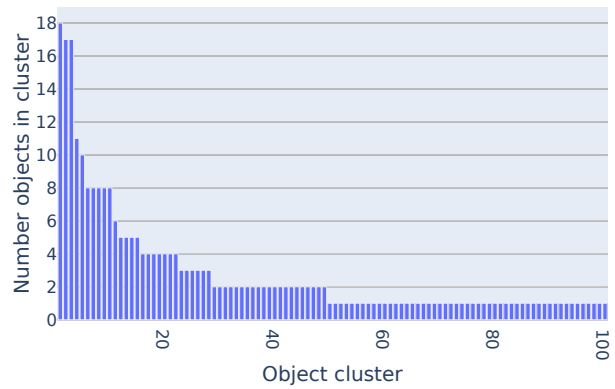
cup, my mug, 9: front door, back door, house door, front door to house, door, my front door, shed door, 10: sunglasses, my wraparound sunglasses, dark glasses, 11: watch, wrist watch, apple watch, apple wath, risk watch, my apple watch, 12: victor stream book reader, orbit braille reader and notetaker, victor reader stream, orbit reader 20 braille display, braillepen slim braille keyboard, braille orbit reader, solo audiobook player, braille note, my braille displat, 13: blue tooth keyboard, bluetooth keyboard, my keyboard, apple wireless keyboard, mini bluetooth keyboard, portable keyboard, keyboard, 14: medication, blister pack of painkillers, tablets, money, aspirin vs tylenol, aspirin, pill bottle, my pill dosette, buckleys, 15: backpack, my work backpack, work bag, bag, shoulder bag, bum bag, back pack, work backpack, 16: slippers, nike trainers, my shoes, boot, trainers, trainer shoe, slipper, 17: reading glasses, glasses, eye glasses, 18: baseball cap, cap, orange skullcap, my tilly hat, hat, my tilly hat upside down, 19: guide dog play cola, dogs lead, guide dog harness, retractable dog lead, leash, guide dog harness, dog lead, dogs, 20: my water bottle, bottle, pop bottle, green water bottle, water bottle, 21: hairbrush, comb, hair brush, 22: adaptive washing machine, washing machine, tumble



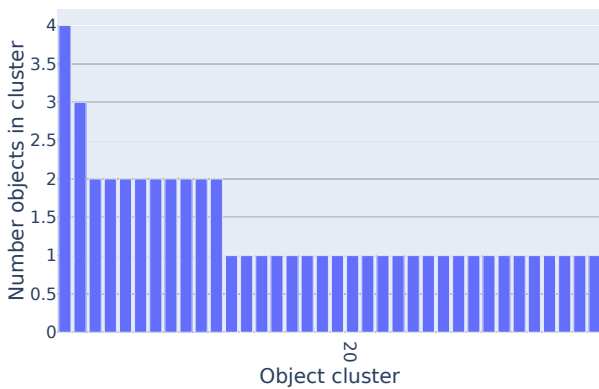
(a) All users (unfiltered dataset)



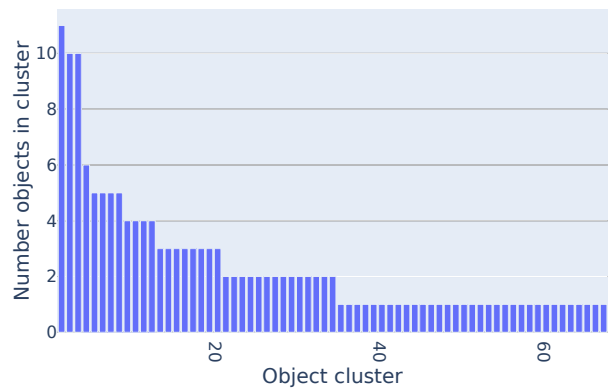
(b) All users (benchmark dataset)



(c) Train users (benchmark dataset)



(d) Validation users (benchmark dataset)



(e) Test users (benchmark dataset)

Figure A.6: Histogram of object clusters (grouped by object similarity) in the ORBIT datasets (benchmark and unfiltered). Objects in each cluster are listed in [Appendix D](#)

dryer, adaptive dryer, 23: digital recorder, dictaphone, pen friend, handheld police scanner, 24: wheely bin, wheelie bin, black bin, recycling bin, bin, 25: face mask, covid mask, my purple mask, blue facemask, 26: screwdriver, small space screwdriver, small screwdriver, spanner, wood phillips head, pex plumbers pliers, 27: 12 measuring cup, 13 measuring cup, 14 measuring cup, 1 cup measuring cup, measuring spoon, 28: lime green marker, yellow marker, pink marker, migenta marker, reptile green marker, 29: airpod pro, single airpod, apple airpods, pro, 30: wireless earphones, bone conducting headset, bose earpods, my muse s headband, 31: phone stand, nobile phone stand, ipod stand, iphone stand, 32: memory stick, usb c dongle, usb stick, usb, 33: scissors, secateurs, 34: socks, sock, 35: necklace, brown leather bracelet, ladies silver bracelet, favourite earrings, 36: microwave, toaster, kettle, one cup kettle, 37: fridge, fridge freezer indicator, 38: prosecco, jd whisky bottle, bottle of alcoholic drink, vagabond ale bottle, 39: digital dab radio, dab radio, speaker, 40: apple phone charger, phone charger, 41: sunglasses case, glasses case, eyewear case, 42: lipstick, chap stick, lip balm, 43: tv unit, flat screen television, tv, smarttv, 44: dining table setup, desk, garden table, 45: liquid level indicator, water level sensor, 46: bottle opener, corkscrew, 47: pint glass, wine glass, glass, 48: lighter, vape pen, cannabis vape battery, 49: pepper shaker, pink himalayan salt, mediterranean sea salt, 50: dog streetball, dog toy, adaptive tennis ball, 51: stylus, apple pencil, 52: mouse, 53: car, 54: local post box, post box, 55: black strappy vest, t-shirts, 56: gloves, winter gloves, 57: hand gel, lotion bottle, 58: perfume, deodorant, 59: tweezers, finger nail clipper, 60: hair clip, headband, 61: inhaler, insulin pen, 62: alcohol wipe, skip prep, 63: my hearing aid, hearing aid, 64: magnifier, pocket magnifying glass, 65: hand saw, 66: tape measure, ruler, 67: electric sanding disc, miter saw, 68: cooker, 69: shelf unit with things, wardrobe, 70: knitting basket, washing basket, basket, 71: stairgate, back patio gate, 72: large sewing needle, knitting needle, 73: mayonnaise jar, mustard, 74: rice, chicken instant noodles, 75: tea, cranberry cream tea, 76: ottawa bus stop, bus stop sign, 77: money clip, 78: headphone case, 79: ps4 controller, 80: my laptop, 81: ipad, 82: compact disc, 83: garden wall, 84: garden shed, 85: litter and dog waste bin, 86: my clock, 87: sleep mask, 88: glasses cleaning wipe, 89: tissue box, 90: condom box, 91: make up, 92: clear nail varnish, 93: toothbrush, 94: eye drops, 95: battery drill, 96: bed, 97: sofa, 98: cushion, 99: mirror, 100: table fan, 101: tred mill, 102: exercise bench, 103: skipping rope, 104: watering can, watering, 105: vase with flowers, 106: veg peeler, 107: sharp knife, 108: wall plug, 109: embroidery thread cone, 110: hole punch, 111: pencil case, 112: paperclips, 113: baked bean tin, 114: banana, 115: mountain dew can, 116: pinesol cleaner, 117: fish food, 118: dog poo, 119: my slate, 120: av tambourine, 121: grinder, 122: journal

Clusters for Figure A.6c [44 train users, 278 objects, 100 clusters] 1: keys, house keys, radar key, my keys, front door keys, keychain, door keys, key, set of keys, 2: remote, tv remote, apple tv remote, amazon remote control, television remote control, remote control, virgin remote control, tv remote control, samsung tv remote control, presentation remote, sky q remote, clickr, fire stick remote, control, television control, remote tv, 3: symbol cane, black mobility cane, my cane, white mobility came, folded white cane, long cane, cane, folded cane, folded long guide cane, p939411 white cane, white came, visibility stick, mobility, mobility cane, white cane, 4: earphones, apple headphones, apple earpods, airpods, my airpod pros case, iphone air pods, airpods pro charging case, airpod case, airpods, my airpods, airpods case, earpods, 5: black small wallet, my purse, my wallet, ladies purse, money pouch, coin purse, wallet for bus pass cards and money, i d wallet, ipod in wallet, walletv, wallet, purse, 6: blue headphones, my headphones, head-phone, bose wireless headphones, headset, my sennheiser pxc 350-2, headphones, 7: phone, mobile phone, iphone 6, apple mobile phone, i phone 11 pro, iphone in case, iphone, cell phone, work phone, phone case, 8: sunglasses, my wraparound sunglasses, dark glasses, 9: medication, blister pack of painkillers, tablets, money, aspirin vs tylenol, aspirin, pill bottle, my pill dosette, buckleys, 10: mug, personal mug, cup again, coffee mug, toddler cup, styrofoam cup, my mug, 11: reading glasses, glasses, eye glasses, 12: slippers, nike trainers, my shoes, boot, trainers, trainer shoe, slipper, 13: watch, wrist watch, apple watch, apple wath, risk watch, my apple watch, 14: backpack, my work backpack, work bag, bag, shoulder bag, bum bag, back pack, work backpack, 15: guide dog play cola, dogs lead, guide dog harness, retractable dog lead, leash, guide dog harness, dog lead, dogs, 16: front door, back door, house door, front door to house, door, my front door, shed door, 17: blue tooth keyboard, bluetooth keyboard, my keyboard, apple wireless keyboard, mini bluetooth keyboard, portable keyboard, keyboard, 18: face mask, covid mask, my purple mask, blue facemask, 19: baseball cap, cap, orange skullcap, my tilly hat, hat, my tilly hat upside down, 20: hairbrush, comb, hair brush, 21: victor stream book reader, orbit braille reader and notetaker, victor reader stream, orbit reader 20 braille display, braillepen slim braille keyboard, braille orbit reader, solo audiobook player, braille note, my braille displat, 22: my water bottle, bottle, pop bottle, green water bottle, water bottle, 23: digital recorder, dictaphone, pen friend, handheld police scanner, 24: memory stick, usb c dongle, usb stick, usb, 25: sun-glasses case, glasses case, eyewear case, 26: fridge, fridge freezer indicator, 27: adaptive washing machine, washing machine, tumble dryer, adaptive dryer, 28: pint glass, wine glass, glass, 29: airpod pro, single airpod, apple airpods, pro, 30: wireless earphones, bone conducting headset, bose earpods, my muse s headband, 31: mouse, 32: apple phone

charger, phone charger, 33: scissors, secateurs, 34: local post box, post box, 35: wheely bin, wheelie bin, black bin, recycling bin, bin, 36: black strappy vest, t-shirts, 37: lip-stick, chap stick, lip balm, 38: alcohol wipe, skip prep, 39: my hearing aid, hearing aid, 40: cooker, 41: microwave, toaster, kettle, one cup kettle, 42: bottle opener, corkscrew, 43: large sewing needle, knitting needle, 44: prosecco, jd whisky bottle, bottle of alcoholic drink, vagabond ale bottle, 45: lighter, vape pen, cannabis vape battery, 46: mayonnaise jar, mustard, 47: rice, chicken instant noodles, 48: tea, cranberry cream tea, 49: ottawa bus stop, bus stop sign, 50: money clip, 51: headphone case, 52: stylus, apple pencil, 53: my laptop, 54: compact disc, 55: digital dab radio, dab radio, speaker, 56: phone stand, nobile phone stand, ipod stand, iphone stand, 57: litter and dog waste bin, 58: socks, sock, 59: gloves, winter gloves, 60: sleep mask, 61: glasses cleaning wipe, 62: tissue box, 63: hand gel, lotion bottle, 64: make up, 65: clear nail varnish, 66: hair clip, headband, 67: toothbrush, 68: inhaler, insulin pen, 69: eye drops, 70: necklace, brown leather bracelet, ladies silver bracelet, favourite earrings, 71: magnifier, pocket magnifying glass, 72: screwdriver, small space screwdriver, small screwdriver, spanner, wood phillips head, pex plumbers pliers, 73: hand saw, 74: battery drill, 75: tape measure, ruler, 76: electric sanding disc, miter saw, 77: tv unit, flat screen television, tv, smarttv, 78: bed, 79: sofa, 80: dining table setup, desk, garden table, 81: mirror, 82: tred mill, 83: exercise bench, 84: skipping rope, 85: stairgate, back patio gate, 86: liquid level indicator, water level sensor, 87: sharp knife, 88: embroidery thread cone, 89: hole punch, 90: pencil case, 91: baked bean tin, 92: banana, 93: pepper shaker, pink himalayan salt, mediterranean sea salt, 94: mountain dew can, 95: fish food, 96: dog poo, 97: dog streetball, dog toy, adaptive tennis ball, 98: av tambourine, 99: grinder, 100: journal

Clusters for Figure A.6d [6 validation users, 50 objects, 36 clusters] 1: keys, house keys, radar key, my keys, front door keys, keychain, door keys, key, set of keys, 2: black small wallet, my purse, my wallet, ladies purse, money pouch, coin purse, wallet for bus pass cards and money, i d wallet, ipod in wallet, walletv, wallet, purse, 3: blue headphones, my headphones, headphone, bose wireless headphones, headset, my sennheiser pxc 350-2, headphones, 4: front door, back door, house door, front door to house, door, my front door, shed door, 5: remote, tv remote, apple tv remote, amazon remote control, television remote control, remote control, virgin remote control, tv remote control, samsung tv remote control, presentation remote, sky q remote, clickr, fire stick remote, control, television control, remote tv, 6: blue tooth keyboard, bluetooth keyboard, my keyboard, apple wireless keyboard, mini bluetooth keyboard, portable keyboard, keyboard, 7: phone, mobile phone, iphone 6, apple mobile phone, i phone 11 pro, iphone in case, iphone, cell phone, work phone, phone case, 8: watch, wrist watch,

apple watch, apple wath, risk watch, my apple watch, 9: sunglasses, my wraparound sunglasses, dark glasses, 10: necklace, brown leather bracelet, ladies silver bracelet, favourite earrings, 11: tv unit, flat screen television, tv, smarttv, 12: apple phone charger, phone charger, 13: car, 14: slippers, nike trainers, my shoes, boot, trainers, trainer shoe, slipper, 15: socks, sock, 16: my clock, 17: condom box, 18: baseball cap, cap, orange skullcap, my tilly hat, hat, my tilly hat upside down, 19: hairbrush, comb, hair brush, 20: perfume, deodorant, 21: tweezers, finger nail clipper, 22: hair clip, headband, 23: backpack, my work backpack, work bag, bag, shoulder bag, bum bag, back pack, work backpack, 24: symbol cane, black mobility cane, my cane, white mobility cane, folded white cane, long cane, cane, folded cane, folded long guide cane, p939411 white cane, white cane, visibility stick, mobility, mobility cane white cane, 25: victor stream book reader, orbit braille reader and notetaker, victor reader stream, orbit reader 20 braille display, braillepen slim braille keyboard, braille orbit reader, solo audiobook player, braille note, my braille displat, 26: magnifier, pocket magnifying glass, 27: guide dog play cola, dogs lead, guide dog harness, retractable dog lead, leash, guide dog harness, dog lead, dogs, 28: shelf unit with things, wardrobe, 29: dining table setup, desk, garden table, 30: vase with flowers, 31: mug, personal mug, cup again, coffee mug, toddler cup, styrofoam cup, my mug, 32: wall plug, 33: paperclips, 34: prosecco, jd whisky bottle, bottle of alcoholic drink, vagabond ale bottle, 35: pinesol cleaner, 36: my slate

Clusters for Figure A.6e [17 test users, 158 objects, 67 clusters] 1: black small wallet, my purse, my wallet, ladies purse, money pouch, coin purse, wallet for bus pass cards and money, i d wallet, ipod in wallet, walletv, wallet, purse, 2: keys, house keys, radar key, my keys, front door keys, keychain, door keys, key, set of keys, 3: remote, tv remote, apple tv remote, amazon remote control, television remote control, remote control, virgin remote control, tv remote control, samsung tv remote control, presentation remote, sky q remote, clickr, fire stick remote, control, television control, remote tv, 4: front door, back door, house door, front door to house, door, my front door, shed door, 5: earphones, apple headphones, apple earpods, airpods, my airpod pro case, iphone air pods, airpods pro charging case, airpod case, airpods, my airpods, airpods case, earpods, 6: victor stream book reader, orbit braille reader and notetaker, victor reader stream, orbit reader 20 braille display, braillepen slim braille keyboard, braille orbit reader, solo audiobook player, braille note, my braille displat, 7: 12 measuring cup, 13 measuring cup, 14 measuring cup, 1 cup measuring cup, measuring spoon, 8: lime green marker, yellow marker, pink marker, magenta marker, reptile green marker, 9: watch, wrist watch, apple watch, apple wath, risk watch, my apple watch, 10: symbol cane, black mobility cane, my cane, white mobility cane, folded white cane, long cane, cane, folded

cane, folded long guide cane, p939411 white cane, white cane, visibility stick, mobility, mobility cane, white cane, 11: screwdriver, small space screwdriver, small screwdriver, spanner, wood phillips head, pex plumbers pliers, 12: mug, personal mug, cup again, coffee mug, toddler cup, styrofoam cup, my mug, 13: blue headphones, my headphones, headphone, bose wireless headphones, headset, my sennheiser pxc 350-2, headphones, 14: blue tooth keyboard, bluetooth keyboard, my keyboard, apple wireless keyboard, mini blue-tooth keyboard, portable keyboard, keyboard, 15: phone, mobile phone, iphone 6, apple mobile phone, i phone 11 pro, iphone in case, iphone, cell phone, work phone, phone case, 16: phone stand, nobile phone stand, ipod stand, iphone stand, 17: wheely bin, wheelie bin, black bin, recycling bin, bin, 18: backpack, my work backpack, work bag, bag, shoulder bag, bum bag, back pack, work backpack, 19: adaptive washing machine, washing machine, tumble dryer, adaptive dryer, 20: my water bottle, bottle, pop bottle, green water bottle, water bottle, 21: airpod pro, single airpod, apple airpods, pro, 22: wireless earphones, bone conducting headset, bose earpods, my muse s headband, 23: digital recorder, dictaphone, pen friend, handheld police scanner, 24: digital dab radio, dab radio, speaker, 25: scissors, secateurs, 26: slippers, nike trainers, my shoes, boot, trainers, trainer shoe, slipper, 27: socks, sock, 28: sunglasses, my wraparound sunglasses, dark glasses, 29: baseball cap, cap, orange skullcap, my tilly hat, hat, my tilly hat upside down, 30: microwave, toaster, kettle, one cup kettle, 31: knitting basket, washing basket, basket, 32: liquid level indicator, water level sensor, 33: pepper shaker, pink himalayan salt, mediterranean sea salt, 34: dog streetball, dog toy, adaptive tennis ball, 35: stylus, apple pencil, 36: ps4 controller, 37: ipad, 38: memory stick, usb c dongle, usb stick, usb, 39: car, 40: garden wall, 41: garden shed, 42: gloves, winter gloves, 43: face mask, covid mask, my purple mask, blue facemask, 44: reading glasses, glasses, eye glasses, 45: hand gel, lotion bottle, 46: hairbrush, comb, hair brush, 47: perfume, deodorant, 48: lipstick, chap stick, lip balm, 49: tweezers, finger nail clipper, 50: medication, blister pack of painkillers, tablets, money, aspirin vs tylenol, aspirin, pill bottle, my pill dosette, buckleys, 51: inhaler, insulin pen, 52: necklace, brown leather bracelet, ladies silver bracelet, favourite earrings, 53: guide dog play cola, dogs lead, guide dog harness, retractable dog lead, leash, guide dog harness, dog lead, dogs, 54: hand saw, 55: tape measure, ruler, 56: electric sanding disc, miter saw, 57: fridge, fridge freezer indicator, 58: cushion, 59: shelf unit with things, wardrobe, 60: dining table setup, desk, garden table, 61: table fan, 62: stairgate, back patio gate, 63: watering can, watering, 64: veg peeler, 65: bottle opener, corkscrew, 66: prosecco, jd whisky bottle, bottle of alcoholic drink, vagabond ale bottle, 67: lighter, vape pen, cannabis vape battery

E. Episodic & non-episodic learning for TORS

In the **(2) personalize** step, a few-shot recognition model, or a TOR, aims to learn to recognize completely new objects from only a few examples, in our case videos, captured by the user themselves. The recognition model can be trained to do this in an episodic or non-episodic manner (i.e. the **(1) train** step). Here, we describe both classes of approach.

For a user κ , we denote that each of their personal objects $p \in \mathcal{P}^\kappa$ has N_p^κ context videos and M_p^κ target videos:

$$\bar{\mathcal{V}}_p^\kappa = \{(\bar{v}_i, p)\}_{i=1}^{N_p^\kappa} \quad \mathcal{V}_p^\kappa = \{(v_i, p)\}_{i=1}^{M_p^\kappa} \quad (1)$$

where \bar{v}_i, v_i are context and target videos respectively, and p is the object label. We group the user’s context and target videos over all their $|\mathcal{P}^\kappa|$ objects as:

$$\bar{\mathcal{V}}^\kappa = \bar{\mathcal{V}}_1^\kappa \cup \dots \cup \bar{\mathcal{V}}_{|\mathcal{P}^\kappa|}^\kappa \quad \mathcal{V}^\kappa = \mathcal{V}_1^\kappa \cup \dots \cup \mathcal{V}_{|\mathcal{P}^\kappa|}^\kappa. \quad (2)$$

E.1. Episodic few-shot learning

An episodic approach [41, 49, 10, 54, 39] is characterized by training the model in “episodes” or tasks. For a train user $\kappa \sim \mathcal{K}^{\text{train}}$, a task is a random sample of context videos \mathcal{C}^κ and target videos \mathcal{T}^κ :

$$\mathcal{C}^\kappa = \{(\bar{v}_i, p_i)\}_{i=1}^N \quad \mathcal{T}^\kappa = \{(v_i, p_i)\}_{i=1}^M \quad (3)$$

where \bar{v}_i, v_i are context and target videos respectively, and $p_i \in \mathcal{P}^\kappa$ is the object label. Note, $\mathcal{C}^\kappa \sim \bar{\mathcal{V}}^\kappa$ and $\mathcal{T}^\kappa \sim \mathcal{V}^\kappa$, where $\bar{\mathcal{V}}^\kappa$ and \mathcal{V}^κ are the total set of the user’s context and target videos, respectively (see Appendix F.2 for further task sampling details).

The few-shot recognition model is trained over many randomly sampled tasks per train user $\kappa \sim \mathcal{K}^{\text{train}}$, typically by maximizing the likelihood of predicting the user’s correct personal object in each frame in a target video $v_f \in \mathcal{V}$, given only that user’s context videos \mathcal{C}^κ :

$$\theta^* = \arg \max_{\theta} \mathbb{E}_{\kappa \sim \mathcal{K}^{\text{train}}} \left[\mathbb{E}_{\substack{\mathcal{C}^\kappa \sim \bar{\mathcal{V}}^\kappa \\ \mathcal{T}^\kappa \sim \mathcal{V}^\kappa}} \left[\mathbb{E}_{(v,p) \sim \mathcal{T}^\kappa} \left[\sum_{v_f \in \mathcal{V}} \log p_{\theta^\kappa}(y_f | v_f, \mathcal{C}^\kappa) \right] \right] \right] \quad (4)$$

where $p_{\theta^\kappa}(y_f | v_f, \mathcal{C}^\kappa)$ is the probability the personalized recognition model f_{θ^κ} assigns to the ground-truth object label for frame v_f . The parameters are typically updated with stochastic gradient descent (SGD) and a cross entropy loss function.

The resulting model f_{θ^*} can be thought of knowing *how* to personalize. That is, for a completely new test user $\kappa \sim \mathcal{K}^{\text{test}}$ in the real-world, θ^* can rapidly be updated to the user’s personalized parameters θ^κ with only a few context videos of that user’s personal objects, \mathcal{C}^κ . The user can then scan f_{θ^κ} around any new target scenario to identify their objects using Eq. (1).

E.2. Non-episodic few-shot learning

A non-episodic approach [51, 46, 5] is characterized by training the model in a standard batch-wise manner. For a train user $\kappa \sim \mathcal{K}^{\text{train}}$, a batch \mathcal{B}^κ is the union of the user’s context and target videos from Eq. (3):

$$\mathcal{B}^\kappa = \mathcal{C}^\kappa \cup \mathcal{T}^\kappa = \{(v_i, p_i)\}_{i=1}^{N+M} \quad (5)$$

where v_i is a context or target video, $p_i \in \mathcal{P}^{\text{all}}$ is the object label, and \mathcal{P}^{all} is the set of personal objects pooled across all users in $\mathcal{K}^{\text{train}}$.

The recognition model is trained over many randomly sampled batches per train user $\kappa \sim \mathcal{K}^{\text{train}}$, typically by maximizing the likelihood of predicting the user’s correct personal object in each frame in a video $v_f \in v$:

$$\theta^* = \arg \max_{\theta} \mathbb{E}_{\kappa \sim \mathcal{K}^{\text{train}}} \left[\mathbb{E}_{\substack{\mathcal{C}^\kappa \sim \mathcal{V}^\kappa \\ \mathcal{T}^\kappa \sim \mathcal{Y}^\kappa}} \left[\mathbb{E}_{(v,p) \sim \mathcal{B}^\kappa} \left[\sum_{v_f \in v} \log p_{\theta}(y_f | v_f) \right] \right] \right] \quad (6)$$

where $p_{\theta}(y_f | v_f)$ is the probability the (generic) model f_{θ} assigns to the ground-truth label $y_f \in \mathcal{P}^{\text{all}}$ for frame v_f . As above, typically SGD and a cross entropy loss are used.

Unlike an episodic approach, the resulting f_{θ^*} is a generic recognizer for all the objects in \mathcal{P}^{all} and does not explicitly know how to personalize. Instead, the generic model is personalized for a new test user $\kappa \sim \mathcal{K}^{\text{test}}$ by fine-tuning f_{θ^*} with the user’s context videos \mathcal{C}^κ of their personal objects. This is equivalent to transfer learning where the (generic) feature extractor is typically frozen, and only a new classifier is learned per user for their objects – together giving the user’s personalized parameters θ^κ . As above, the user can then scan f_{θ^κ} around to predict the object in target frames using Eq. (1).

F. Implementation Details

F.1. Baselines

ProtoNets [41]. ProtoNets is a metric-based few-shot learner where a task’s target frames are classified based on how close (typically as squared Euclidean distance) the target frame embedding is to each of the mean embeddings for each object class in the task’s context videos. We use a ResNet18 [15] feature extractor that is pre-trained on ImageNet [40]. We then train episodically on T^{train} tasks per train user drawn from $\mathcal{K}^{\text{train}}$ with a learning rate of 10^{-4} (reduced by 0.1 for the feature extractor). We evaluate the trained model on all target videos in T^{test} tasks per test user in $\mathcal{K}^{\text{test}}$, and report the metrics over \mathcal{T}^{all} , the flattened set of all target videos across all tasks for all test users.

CNAPs [39]. CNAPs is a model-based few-shot learner where a task’s target frames are classified by a model *generated* with 1 forward pass of the task’s context videos through

a hypernet. In practice, the hypernet generates only a subset of the model’s parameters following [39] – the task’s classifier and *FiLM* adapters [36] which are placed after convolution blocks in the feature extractor. We use a ResNet18 [15] feature extractor that is pre-trained on ImageNet [40] and kept frozen. We train the hypernet episodically on T^{train} tasks per train user drawn from $\mathcal{K}^{\text{train}}$ with a learning rate of 10^{-4} (reduced by 0.1 for the feature extractor). We evaluate the trained model on all target videos in T^{test} tasks per test user in $\mathcal{K}^{\text{test}}$, and report the metrics over \mathcal{T}^{all} .

MAML [10]. MAML is a optimization-based few-shot learner where a task’s target frames are classified after the model has taken G gradient steps, computed based on the loss of the task’s context videos. We use a ResNet18 [15] feature extractor that is pre-trained on ImageNet [40]. We then train episodically on T^{train} tasks per train user drawn from $\mathcal{K}^{\text{train}}$ with an inner and outer learning rate of 10^{-3} and 10^{-5} , respectively (reduced by 0.1 for the feature extractor). We evaluate the trained model on all target videos in T^{test} tasks per test user in $\mathcal{K}^{\text{test}}$, and report the metrics over \mathcal{T}^{all} . Note that since each (train and test) task can have a different number of objects, we append a new classifier per task, initialized with zeroes following [48]. The classifier is therefore not learned, but instead the result after G gradient steps. At both train and test time, $G = 15$.

FineTuner [46, 5]. FineTuner is a non-episodic few-shot learner where a task’s target frames are classified by a model whose classifier has been finetuned using the task’s context videos, while the feature extractor is fixed. This is equivalent to a transfer learning approach. We use a ResNet18 [15] feature extractor that is pre-trained on ImageNet [40]. Following [46, 5], we first tune this feature extractor using $\mathcal{K}^{\text{train}}$: we pool the personal objects across *all* train users in $\mathcal{K}^{\text{train}}$ and train a standard classification model⁷ using T^{train} tasks per train user. Because the model is non-episodic, the context and target videos of each task are pooled and treated as a standard batch, following Eq. (5). We use the Adam optimizer [21] and a learning rate of 10^{-4} (reduced by 0.1 for the feature extractor). At test time, this feature extractor is frozen, and for each task sampled for a test user drawn from $\mathcal{K}^{\text{test}}$, a new classifier is appended, initialized with zeroes following [48] and tuned for $G = 50$ gradient steps using the task’s context videos and a learning rate of 0.1. We evaluate the trained model on all target videos in T^{test} tasks per test user in $\mathcal{K}^{\text{test}}$, and report the metrics over \mathcal{T}^{all} .

F.2. Sampling tasks

The only strict requirement of the ORBIT evaluation protocol is that at meta-testing, a model outputs a prediction for every frame from every target video for every test user. How tasks are sampled from context/target videos during

⁷Because there are similar objects across the train users, we use the objects’ cluster labels (i.e. 122-way classification task), as in Figure A.6b

training, and context videos during testing is otherwise flexible. In this section, we detail how we sample tasks, but acknowledge that other strategies could be chosen.

Train user tasks We sample T^{train} tasks for each train user $\kappa \sim \mathcal{K}^{\text{train}}$ as follows:

1. **Way:** sample a set of the user’s objects $\ddot{\mathcal{P}}^\kappa \sim \mathcal{P}^\kappa$
2. **Shot:** for each object $p \in \ddot{\mathcal{P}}^\kappa$, sample $n_p \sim [1, \dots, N_p^\kappa]$ and $m_p \sim [1, \dots, M_p^\kappa]$ ⁸
3. Construct context set $\mathcal{C}^\kappa = \{(\bar{v}, p) \stackrel{n_p}{\sim} \bar{\mathcal{V}}_p^\kappa \mid \forall p \in \ddot{\mathcal{P}}^\kappa\}$
4. Construct target set $\mathcal{T}^\kappa = \{(v, p) \stackrel{m_p}{\sim} \mathcal{V}_p^\kappa \mid \forall p \in \ddot{\mathcal{P}}^\kappa\}$

For memory reasons, during training we impose a video cap per object of $n_p = 5$ and $m_p = 4$ if $|\ddot{\mathcal{P}}^\kappa| \geq 6$, otherwise the caps are doubled, and an object cap of $|\ddot{\mathcal{P}}^\kappa| = 10$.

Test user tasks We sample T^{test} tasks for each test user $\kappa \sim \mathcal{K}^{\text{test}}$ as follows:

1. **Way:** select *all* the user’s objects, $\ddot{\mathcal{P}}^\kappa = \mathcal{P}^\kappa$ (i.e. test personalization for all objects)
2. **Shot:** for each object $p \in \ddot{\mathcal{P}}^\kappa$, $n_p = N_p^\kappa$ and $m_p = M_p^\kappa$ (i.e. use all context and target videos)⁸
3. Construct context set $\mathcal{C}^\kappa = \{(\bar{v}, p) \stackrel{n_p}{\sim} \bar{\mathcal{V}}_p^\kappa \mid \forall p \in \ddot{\mathcal{P}}^\kappa\}$
4. Construct target set $\mathcal{T}^\kappa = \{(v, p) \stackrel{m_p}{\sim} \mathcal{V}_p^\kappa \mid \forall p \in \ddot{\mathcal{P}}^\kappa\}$

For testing, the only cap we impose is $n_p = 5$ if $|\ddot{\mathcal{P}}^\kappa| \geq 6$, otherwise the cap is doubled.

F.3. Task sampling hyper-parameters

The number of tasks per train user was selected over a range of 5 to 500 (see Table A.7). The number of tasks per test user was selected to reduce variance in the reported metrics. The number of clips per video and the clip length were selected based on available GPU memory during training/testing (2× Dell NVIDIA Tesla V100 32GB GPU).

- Tasks per train user, $T^{\text{train}} = 50$
- Tasks per test user, $T^{\text{test}} = 5$
- Clip length, $L = 8$ frames
- Clips per context video in a train task, $S_{\mathcal{C}}^{\text{train}} = 4$
- Clips per target video in a train task, $S_{\mathcal{T}}^{\text{train}} = 4$
- Clips per context video in a test task, $S_{\mathcal{C}}^{\text{test}} = 8$

F.4. Optimization hyper-parameters

The learning rates were selected with a grid search over the range 10^{-5} to 10^{-1} . For all baselines, we use the Adam optimizer [21] with default parameters $\beta=(0.9, 0.999)$, $\epsilon = 10^{-8}$, and no weight decay.

G. Extended analyses

Here we extend analyses from Section 5.2 in the main paper.

Meta-training on other few-shot datasets. Table A.3 shows the results when meta-training on Meta-Dataset and meta-testing on the ORBIT benchmark, using each of the baseline models (extends Table 6 in the main paper).

User-centric vs user-agnostic training. ORBIT proposes a user-centric training strategy where each task is sampled from only one train user’s objects. We compare this to a user-agnostic approach in Table A.4 where we pool objects across *all* train users in $\mathcal{K}^{\text{train}}$ and construct train tasks from objects randomly sampled from this pool (keeping all other sampling procedures the same). A user-agnostic approach is more common in typical few-shot learning pipelines. Performance between the two is overall equivalent, suggesting that imposing a user-centric hierarchy on the task sampling does not negatively impact performance, relative to imposing no hierarchy.

Per-user performance. We plot CLU-VE frame accuracy, frames-to-recognition and video accuracy per user, for all baseline models in Figure A.9. Here, we see the same trend as Figure 4 in the main paper — personalization performance varies widely across users.

Train task composition. In Figures 5 and 6 in the main paper, we investigate the impact of the number of context videos per object, and the number of objects per user on CLU-VE frame accuracy, respectively. We extend these plots to the frames-to-recognition and video accuracy metrics in Figure A.7 and Figure A.8 and complement them with their corresponding tables in Tables A.5 and A.6.

Number of tasks per train user. We investigated the impact of the number of tasks sampled per train user, T^{train} during meta-training, and found that CLU-VE performance increases with more tasks, but levels off around 50 tasks per user (Table A.7). We expect that bigger gains could be achieved by accounting for the informativeness of frames, instead of uniform sampling. This is likely because many clean and clutter videos are noisy and contain redundant frames.

⁸Note, N and M in Eq. (3) and Eq. (5) are $N = \sum_{p \in \ddot{\mathcal{P}}^\kappa} n_p$ and $M = \sum_{p \in \ddot{\mathcal{P}}^\kappa} m_p$, respectively

MODEL	Clean Video Evaluation (CLE-VE)			Clutter Video Evaluation (CLU-VE)		
	FRAME ACC	FTR	VIDEO ACC	FRAME ACC	FTR	VIDEO ACC
ProtoNets [41]	54.97 (2.33)	13.50 (1.99)	68.36 (3.17)	42.53 (1.81)	22.34 (1.76)	48.67 (2.53)
CNAPs [39]	45.35 (2.60)	26.72 (2.67)	53.09 (3.41)	33.95 (1.93)	42.40 (2.33)	35.07 (2.41)
MAML [10]	28.64 (2.65)	53.94 (3.27)	30.79 (3.15)	23.73 (1.86)	62.76 (2.32)	24.07 (2.16)
FineTuner [46, 5]	56.46 (2.37)	13.97 (2.06)	70.42 (3.11)	44.73 (1.87)	22.67 (1.81)	48.27 (2.53)

Table A.3: Models perform poorly when meta-trained on Meta-Dataset and meta-tested on ORBIT, suggesting that existing few-shot datasets may be insufficient for real-world adaptation. Results are reported as the average (95% confidence interval) over all target videos across all tasks for 17 test users.

MODEL	Clean Video Evaluation (CLE-VE)			Clutter Video Evaluation (CLU-VE)		
	FRAME ACC	FTR	VIDEO ACC	FRAME ACC	FTR	VIDEO ACC
ProtoNets [41]	65.56 (2.13)	6.07 (1.12)	77.21 (2.86)	48.58 (1.76)	17.30 (1.61)	56.67 (2.51)
CNAPs [39]	64.19 (2.29)	8.08 (1.42)	73.82 (3.00)	51.12 (1.86)	17.93 (1.68)	56.47 (2.51)
MAML [10]	66.13 (2.38)	11.02 (1.89)	74.30 (2.98)	48.69 (1.93)	21.97 (1.90)	52.53 (2.53)
FineTuner [46, 5]	69.05 (2.31)	10.06 (1.79)	80.24 (2.72)	52.91 (1.86)	17.10 (1.66)	57.53 (2.50)

Table A.4: User-agnostic training on the ORBIT dataset (i.e. train tasks are sampled from objects pooled across *all* train users in $\mathcal{K}^{\text{train}}$) performs equally well to user-centric training. Results are reported as the average (95% confidence interval) over all target videos across all tasks for 17 test users.

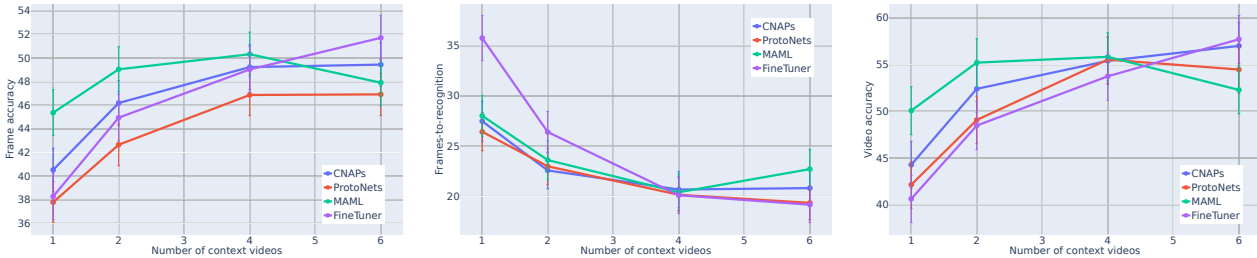


Figure A.7: Meta-training with more context videos per object leads to better CLU-VE performance (frame accuracy - left; frames-to-recognition - center; video accuracy - right). Frames are sampled from an increasing number of clean videos per object using the number of clips per video (S^{train}) to keep the total number of context frames fixed in train tasks. Extends Figure 5 in the main paper.

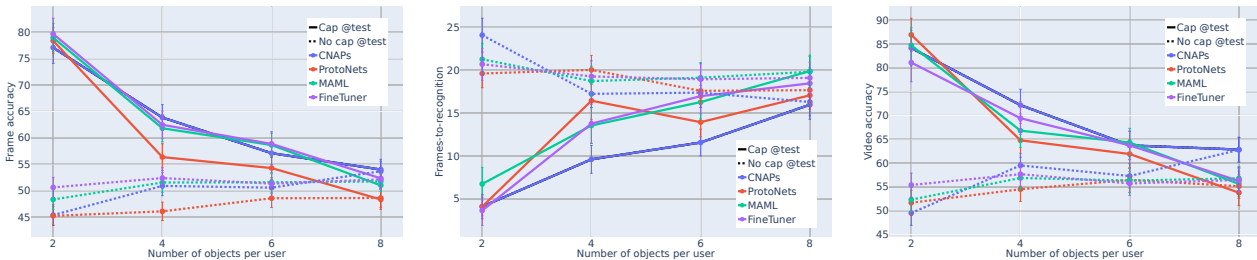
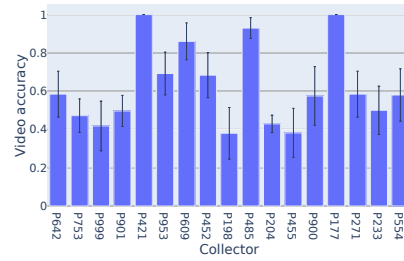
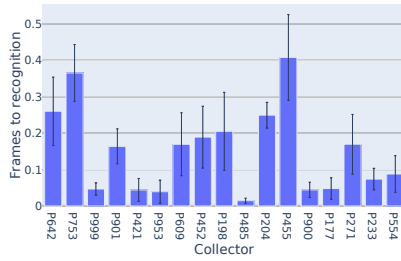
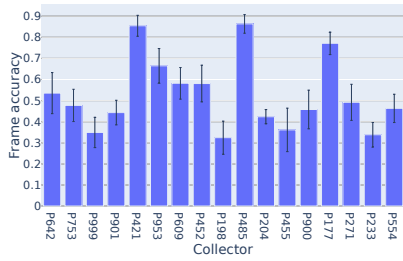
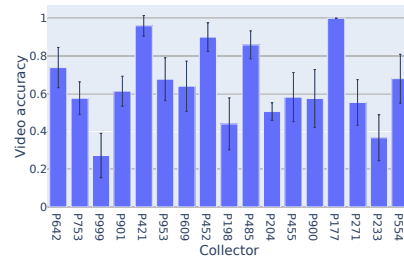
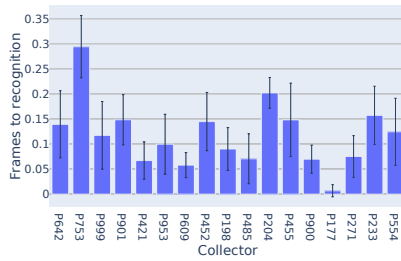
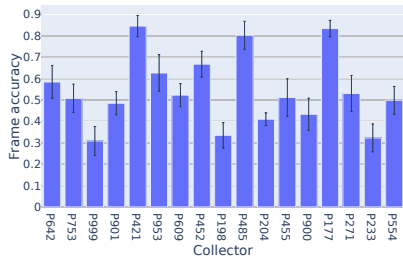


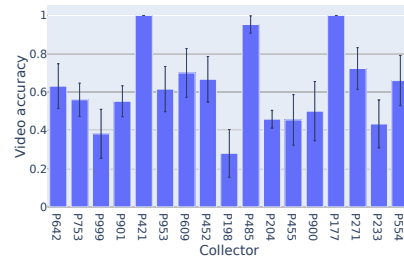
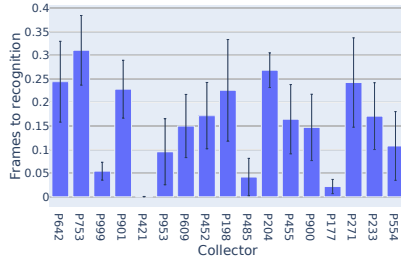
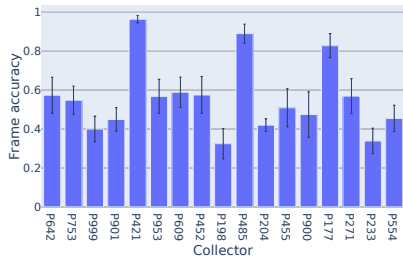
Figure A.8: Meta-training and -testing with more objects per user poses a harder recognition problem (solid line), however meta-training with fewer objects than encountered at meta-testing (dashed line) shows only a small performance drop in CLU-VE compared to Table 5, suggesting that models may be able to adapt to more objects in the real-world (frame accuracy - left; frames-to-recognition - center; video accuracy - right). Extends Figure 6 in the main paper.



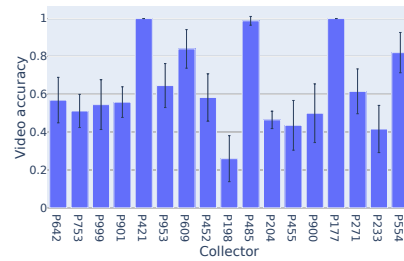
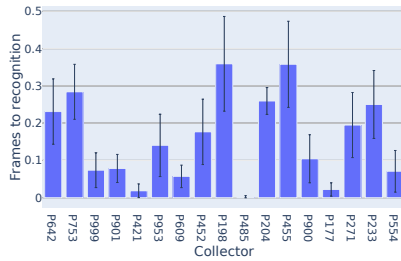
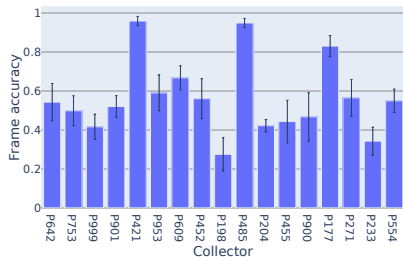
(a) Results with CNAPs [39]



(b) Results with ProtoNets [41]



(c) Results with MAML [10]



(d) Results with FineTuner [46, 5]

Figure A.9: CLU-VE performance varies widely per test user across all metrics and all baseline models. Error bars are 95% confidence intervals.

N_p^κ	S_C^{train}	L	FRAME ACC	FTR	VIDEO ACC
1	12	8	40.53 (1.84)	27.49 (2.00)	44.27 (2.51)
2	6	8	46.19 (1.89)	22.59 (1.83)	52.40 (2.53)
4	3	8	49.23 (1.88)	20.69 (1.80)	55.40 (2.52)
6	2	8	49.44 (1.85)	20.83 (1.78)	57.00 (2.51)

(a) Results with CNAPs [39]

N_p^κ	S_C^{train}	L	FRAME ACC	FTR	VIDEO ACC
1	12	8	37.79 (1.72)	26.44 (1.91)	42.13 (2.50)
2	6	8	42.66 (1.78)	23.00 (1.82)	49.07 (2.53)
4	3	8	46.87 (1.76)	20.17 (1.70)	55.53 (2.51)
6	2	8	46.92 (1.79)	19.36 (1.67)	54.47 (2.52)

(b) Results with ProtoNets [41]

N_p^κ	S_C^{train}	L	FRAME ACC	FTR	VIDEO ACC
1	12	8	45.37 (1.94)	28.03 (2.02)	50.07 (2.58)
2	6	8	49.04 (1.90)	23.62 (1.91)	55.21 (2.57)
4	3	8	50.32 (1.88)	20.42 (1.81)	55.83 (2.56)
6	2	8	47.91 (1.95)	22.72 (1.92)	52.29 (2.58)

(c) Results with MAML [10]

N_p^κ	S_C^{train}	L	FRAME ACC	FTR	VIDEO ACC
1	12	8	38.28 (1.98)	35.76 (2.25)	40.62 (2.54)
2	6	8	44.95 (1.97)	26.41 (2.06)	48.47 (2.58)
4	3	8	49.03 (1.92)	20.12 (1.83)	53.75 (2.58)
6	2	8	51.71 (1.89)	19.18 (1.78)	57.71 (2.55)

(d) Results with FineTuner [46, 5]

Table A.5: More context videos per object leads to better CLU-VE performance. Frames are sampled from an increasing number of videos per object (N_p^κ) using the number of clips per context video (S_C^{train}) to keep the total number of context frames fixed in train tasks. Corresponds to Figure 5 in the main paper.

#objs/ train user	#objs/ test user	FRAME ACC	FTR	VIDEO ACC
2	2	77.08 (2.98)	4.10 (1.41)	84.17 (3.77)
4	4	63.85 (2.45)	9.61 (1.61)	72.17 (3.34)
6	6	57.10 (2.14)	11.57 (1.57)	63.72 (2.99)
8	8	54.00 (1.96)	15.97 (1.69)	62.84 (2.62)
2	no-cap	45.38 (1.94)	24.08 (1.97)	49.51 (2.58)
4	no-cap	50.91 (1.85)	17.24 (1.62)	59.51 (2.54)
6	no-cap	50.57 (1.89)	17.38 (1.69)	57.29 (2.55)
8	no-cap	53.68 (1.90)	16.29 (1.63)	62.78 (2.50)

(a) Results with CNAPs [39]

#objs/ train user	#objs/ test user	FRAME ACC	FTR	VIDEO ACC
2	2	78.38 (2.45)	4.10 (1.08)	86.94 (3.48)
4	4	56.36 (2.53)	16.44 (2.22)	64.78 (3.56)
6	6	54.28 (2.09)	13.94 (1.71)	61.91 (3.02)
8	8	48.34 (1.87)	17.07 (1.64)	53.79 (2.71)
2	no-cap	45.24 (1.75)	19.61 (1.66)	51.67 (2.58)
4	no-cap	46.09 (1.75)	20.03 (1.69)	54.51 (2.57)
6	no-cap	48.57 (1.76)	17.59 (1.61)	56.46 (2.56)
8	no-cap	48.62 (1.77)	17.67 (1.61)	55.14 (2.57)

(b) Results with ProtoNets [41]

#objs/ train user	#objs/ test user	FRAME ACC	FTR	VIDEO ACC
2	2	78.98 (2.69)	6.74 (1.94)	84.72 (3.72)
4	4	61.82 (2.59)	13.55 (2.11)	66.81 (3.51)
6	6	58.64 (2.27)	16.28 (1.96)	64.32 (2.98)
8	8	51.01 (1.99)	19.89 (1.87)	55.63 (2.70)
2	no-cap	48.34 (1.84)	21.27 (1.79)	52.33 (2.53)
4	no-cap	51.55 (1.89)	18.73 (1.73)	56.87 (2.51)
6	no-cap	51.59 (1.87)	19.12 (1.75)	56.33 (2.51)
8	no-cap	51.75 (1.87)	19.81 (1.78)	56.80 (2.51)

(c) Results with MAML [10]

#objs/ train user	#objs/ test user	FRAME ACC	FTR	VIDEO ACC
2	2	79.68 (2.97)	3.65 (1.73)	81.11 (4.04)
4	4	62.47 (2.61)	13.77 (2.27)	69.42 (3.44)
6	6	58.86 (2.31)	16.97 (2.06)	63.72 (2.99)
8	8	52.34 (2.00)	18.46 (1.87)	56.25 (2.69)
2	no-cap	50.62 (1.90)	20.69 (1.85)	55.40 (2.52)
4	no-cap	52.39 (1.92)	19.27 (1.80)	57.67 (2.50)
6	no-cap	51.33 (1.88)	18.94 (1.78)	55.73 (2.51)
8	no-cap	52.14 (1.90)	19.10 (1.78)	56.47 (2.51)

(d) Results with FineTuner [46, 5]

Table A.6: Meta-training and -testing with more objects per user poses a harder recognition problem, however meta-training with fewer objects than encountered at meta-testing shows only a small performance drop in CLU-VE compared to Table 5, suggesting that models may be able to adapt to more objects in the real-world. Corresponds to Figure 6 in the main paper.

T^{train}	FRAME ACC	FTR	VIDEO ACC
5	48.08 (1.85)	22.21 (1.84)	55.07 (2.52)
25	52.11 (1.85)	17.37 (1.62)	59.27 (2.49)
50	50.44 (1.88)	19.88 (1.74)	56.67 (2.51)
100	51.24 (1.86)	18.96 (1.71)	59.53 (2.48)
200	50.83 (1.82)	20.25 (1.72)	60.20 (2.48)
500	49.72 (1.81)	18.83 (1.69)	56.07 (2.51)

(a) Results with CNAPs [39]

T^{train}	FRAME ACC	FTR	VIDEO ACC
5	43.90 (1.71)	19.42 (1.63)	49.07 (2.53)
25	46.89 (1.76)	20.40 (1.72)	54.00 (2.52)
50	50.92 (1.72)	16.39 (1.50)	60.87 (2.47)
100	49.59 (1.79)	19.38 (1.64)	59.33 (2.49)
200	49.78 (1.74)	15.51 (1.46)	58.20 (2.50)
500	48.70 (1.79)	18.28 (1.61)	54.67 (2.52)

(b) Results with ProtoNets [41]

T^{train}	FRAME ACC	FTR	VIDEO ACC
5	44.33 (2.05)	32.60 (2.20)	47.27 (2.53)
25	51.52 (1.89)	19.16 (1.75)	57.33 (2.50)
50	51.67 (1.86)	19.74 (1.76)	57.47 (2.50)
100	51.64 (1.86)	20.09 (1.80)	56.87 (2.51)
200	50.61 (1.92)	21.64 (1.85)	56.13 (2.51)
500	49.78 (1.89)	21.86 (1.84)	56.27 (2.51)

(c) Results with MAML [10]

T^{train}	FRAME ACC	FTR	VIDEO ACC
5	48.99 (1.82)	19.32 (1.75)	56.47 (2.51)
25	51.90 (1.87)	19.71 (1.81)	58.13 (2.50)
50	52.52 (1.88)	18.60 (1.76)	58.00 (2.50)
100	52.20 (1.89)	17.99 (1.72)	57.13 (2.50)
200	54.79 (1.87)	16.86 (1.67)	61.13 (2.47)
500	52.90 (1.88)	18.18 (1.74)	57.87 (2.50)

(d) Results with FineTuner [46, 5]

Table A.7: Sampling more tasks per train user has limited benefits on CLU-VE performance beyond $T^{\text{train}} = 50$ suggesting that sampling techniques that account for frame informativeness may be required.